AN EAR FLOW CHAMBER FOR STUDYING TYMPANOSTOMY TUBE OCCLUSION

By

ETHAN GLENN SHERMAN

A THESIS PRESENTED TO THE GRADUATE SCHOOL
OF THE UNIVERSITY OF FLORIDA IN PARTIAL FULFILLMENT
OF THE REQUIREMENTS FOR THE DEGREE OF
MASTER OF ENGINEERING

UNIVERSITY OF FLORIDA

2005

This document is dedicated to my mother and father for the unwavering support they have given me throughout my life and to my one and only love Amy who is my life.

ACKNOWLEDGMENTS

I would like to thank my fiancée, Amy, and my parents for all of the support they have given me throughout the years. I would also like to thank Dr. Roger Tran-Son-Tay for guiding me through this process and for the wonderful opportunities I have received. In addition I would like to thank my supervisory committee Dr. Malisa Sartinoranont and Dr. Patrick Antonelli for their encouragement and enthusiasm throughout this process. I would also like to extend my gratitude to the members of my lab Cecile, Brent, Eddy, Darren, Maties, Chessy, Jessica, Kori, Tiali, and Jompo. I thank them for their help and guidance as colleagues and friends.

TABLE OF CONTENTS

LIST OF TABLES

LIST OF FIGURES

Abstract of Thesis Presented to the Graduate School
of the University of Florida in Partial Fulfillment of the
Requirements for the Degree of Master of Engineering

AN EAR FLOW CHAMBER FOR STUDYING TYMPANOSTOMY TUBE OCCLUSION

By

Ethan Glenn Sherman

August 2005

Chair: Roger Tran-Son-Tay
Major Department: Mechanical and Aerospace Engineering

The most common treatment in the United States for relieving symptoms of otitis media is tymponostomy tubes. However, despite their effectiveness, there are some drawbacks in their design, mostly tube plugging. Approximately 20% of the tubes become occluded after implantation, causing additional pain and suffering. These complications suggest that variations in the length, composition, and coatings of the tubes may influence their effectiveness.

The objective of this research is to develop an in-vitro model of the ear that will enable testing of parameters involved in tube plugging. Previous in-vitro ear chamber designs consisted of a vertical cylinder holding an occluded tympanostomy tube. Gravity then pushes a solvent fluid through the occlusion. However, this design did not allow for the study of the real-time formation and removal of the occlusion. This thesis will specifically focus on the cause of tube plugging as a result of measuring the flow of mucus and air through the tube. The new chamber consists of an enclosed Lexan channel

with a fluid-filled syringe at one end, an air-filled syringe in the center and a tympanostomy tube at the exit. The fluid-filled syringe models the continuous supply of mucus produced by the body in response to infection, while the air-filled syringe models the natural function of the Eustachian tube. The unique function of this model is that the system is continuously monitoring the force required to push the mucus and air through the tube allowing for real time analysis of tube plugging. Therefore, as the tube becomes occluded the force required to push the fluid through the tube increases. The results stated that the new in-vitro chamber design can be used to model the formation of occlusions.

CHAPTER 1
INTRODUCTION

Tympanostomy tubes (TT) are devices that are inserted into the tympanic membrane to relieve pressure and otitis media from behind the ear drum. They consist of a length of tube that has a flange at one or both ends. The flange is designed to secure the tube in place during operation.

Tympanostomy tubes have been around for almost 250 years with the earliest forms dating back to the 1760s. Since then, the most significant breakthrough came in the 1940s with Armstrong [1], who was the first to use plastic tubes and set the standard for designing and implanting the devices. Today tympanostomy tubes come in a wide variety of shapes, sizes, and compositions, but they still hold true to the original flange and tube design [2].

Ear infections caused by the buildup of otitis media are the leading cause of hearing loss in children and the most widespread reason for a child to be given an anesthetic [3,4]. The most common treatment for relieving symptoms of ear infections are tympanostomy tubes (vent tubes) [3]. They can be implanted during outpatient surgery and can remain in the ear for as long as 18 months [2]. However, despite their effectiveness there is still some drawbacks in the design, most importantly tube plugging. Tympanostomy tubes have been shown to become occluded in 1.4-36% of cases. This results in additional pain and suffering as well as absences from school and parents missing work [4-6].

Objective

There has been extensive research regarding ways to decrease the percentage of tube occlusion [1-23] by using vasoconstrictors, ointments, and various tube compositions. However, the majority of these studies have used patients, and therefore, the results are limited to the number of subjects the researchers can obtain for each study. For this reason there is a need for an in-vitro experiment that can mimic the environment of the ear in which to study the tube plugging phenomenon. The objective of this research is to develop an in-vitro model of the ear that will enable testing of parameters involved in tube plugging. This thesis will specifically focus on the fabrication of the flow system used to measure the formation of occlusions.

Specific Aims

The specific aims of this thesis are as follows:

- To design and build a chamber that will model the flow environment within the middle and outer ear.
- To design and build a system for autonomously controlling the data acquisition, and fluid flow within the chamber.
- To test the flow chamber by analyzing the formation of tube plugging as a function of length.

CHAPTER 2
BACKGROUND

Ear Anatomy

A recent publication by Rovers et al. [17] states that by the age of 3 almost every child has experienced some form of otitis, either acute otitic media (AOM), or otitis media with effusion (OME), with most cases ending with spontaneous resolution. In fact, 50-85% of children by age 3 have had (AOM), with the majority of incidences occurring between 6 and 11 months. In addition, 10-20% of children have recurrent AOM (>2 occurrences), with 40% of them having more than 6 incidents. According to the National Institute of Health, one third of all pediatric visits are the result of ear infections. Plus, ear infections are also the most frequent reason for a child to undergo general anesthesia [4]. The annual cost in the United States alone is $3-5 billion for middle ear related infections [14, 17]. With such high occurrence rates, otitis media (OM) appears to be as familiar as the common cold and is part of the development of a child's immune system.

Ottis media follows two stages, the acute and effusion stage. Acute ottic media appears as a middle ear effusion (MEE), with signs of otalgia, otorrhoea, fever, or irritability. Ottitis media with effusion is a MEE without the signs of acute otitis [17]. Both conditions appear to be the result of abnormalities from anatomic or physiological changes in the Eustachian tube, infection, or allergy.

The most universal treatment for removing the symptomatic otitis media is the use of tympansotomy (ventilation) tubes (TT) (Figure 2-1). This operation is performed over one million times per year [14]. The purpose of the tympanostomy tube is to provide

continuous ventilation of the middle ear as well as to provide a method of expulsion of the otitis media (OM) [6].

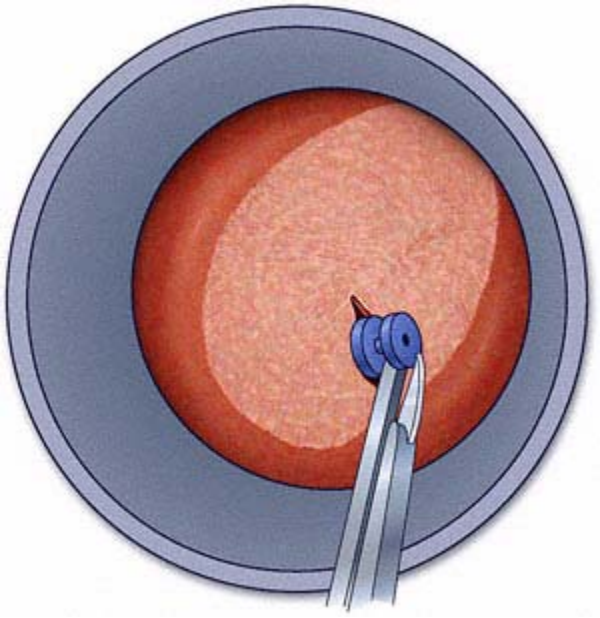

Figure 2-1: Schematic of tympanostomy tube being inserted into a tympanic membrane.

The advantages of this device are to prevent hearing loss, reduce the quantity of acute otitis media (AOM), and reverse hyperplasia in the middle ear. Therefore, there is less need to visit the doctor, less time lost from work or school, and a drop off in the need for antibiotics [5].

The ear's main functions are for hearing and balance. Its structure is divided into three sections: the outer, middle, and inner ear (Figure 2-2). The outer ear consists of the auricle which is the shell-shaped projection that surrounds the external auditory canal. The function of the auricle is to focus sound into the external auditory canal. This canal is a curved tube that extends from the outer ear to the eardrum. The canal consists of elastic cartilage at the auricle end and the remaining part is cut into the temporal bone. The entire canal is covered with skin as well as hairs, sebaceous glands, and ceruminous

glands. Ceruminous glands secrete a yellow-brown cerumen or earwax which traps foreign bodies and repels insects (Figure 2-2).

Sound from the external auditory canal is focused onto the tympanic membrane or eardrum. The eardrum is the boundary between the outer ear and the middle ear and is composed of a thin, translucent, connective tissue membrane. It is shaped into a cone with the peak facing medially. The medial side is covered by a layer of mucus and the lateral side is covered by skin. As sound hits the eardrum it vibrates and this vibration is transferred to the bones of the middle ear (Figure 2-2).

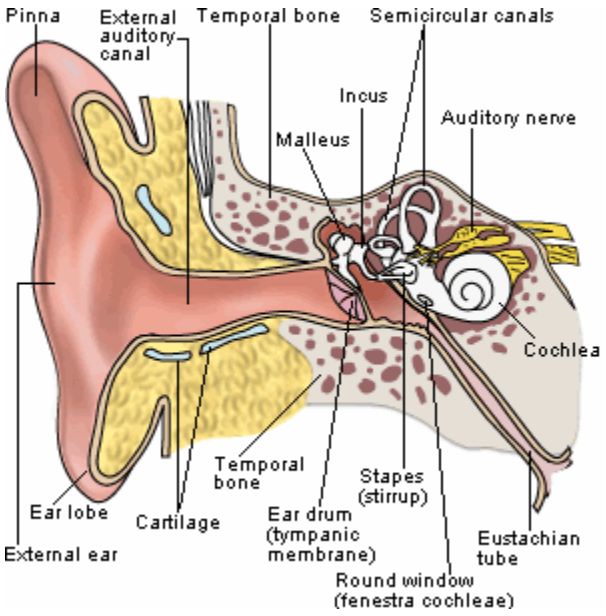

Figure 2-2: Ear structure.

An infection in the ear usually occurs in the middle ear and is the result of inadequate Eustachian tube function and immune response. The middle ear is a cavity that borders the eardrum on the lateral side and the superior oval window and inferior round window on the medial side (Figure 2-2, Figure 2-3). This cavity is filled with air and is lined with mucus. The middle ear consists of the epitympanic recess located superiorly in the cavity and contains the mastoid antrum, which is a canal that

communicates with the mastoid air cells in the mastoid process. On the anterior side of the cavity is the pharyngotympanic tube (Eustachian tube). This tube connects the middle ear to the nasopharynx in the throat. The eustachian tube functions as a pressure equalizer between the outside atmospheric pressure and the inner ear pressure and draws off excess fluid from the middle ear. During normal operation it is closed and flat. However, swallowing or yawning can open the tube briefly to equalize the pressure. Pressure balance is important because the eardrum cannot vibrate effectively if the pressure is greater on one side than the other. The membrane tends to bulge which can distort sound and can cause hearing loss and pain (Figure 2-1). The remaining structures of the middle and inner ear are designed to translate the motion of the ear drum to the various auditory regions. In addition, they function to maintain balance and relay body position to the brain [24].

Since the 1950's typanostomy tubes have been used to relieve inner ear pressure and other symptoms of otitis media. A typical tube consists of a long cylinder with a bulge or flange at one end. Unfortunately, the many designs and various compositions that are used to create this tube have varying success rates. Modern science, however, has developed ways to improve on the common design with various coatings, composites, and geometrical configurations.

The cause of ear infections is a topic of much research. It is believed to be mainly due to microbial load and immune response. Other significant factors are age, genetic predisposition, Eustachian tube malfunction, older siblings with infections, day care, time of year, and second hand smoke [14].

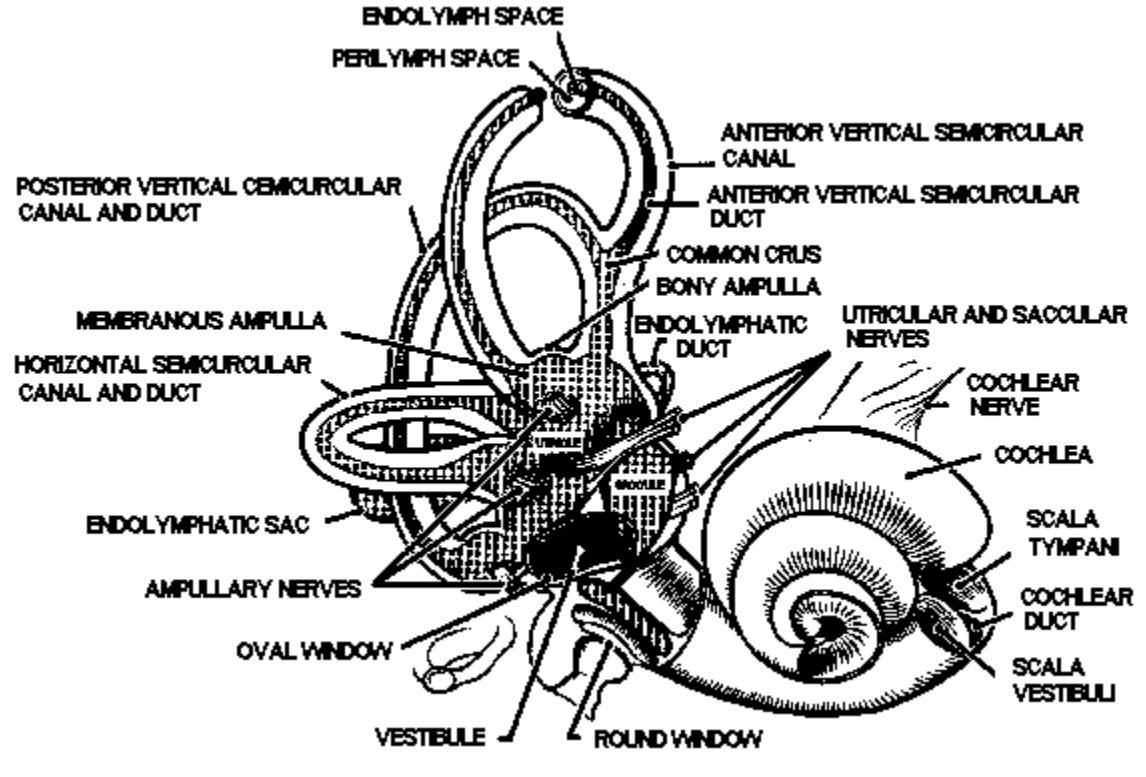

Figure 2-3: Inner ear structure.

An ear infection may start with a common upper respiratory infection which causes congestion of the nasopharynx and Eustachian tube. The tube malfunctions resulting in excess pressure and mucus. Following this, pathogens can be aspirated into the middle ear, which stimulates an inflammatory immune response. If left untreated the consequences can include perforation of the ear drum, mastoiditis, facial paralysis, external otitis, loss of balance, and motor dysfunction [17].

Occlusion Treatment

Despite all the advantages provided by tympanostomy tubes, there is still one significant drawback in the design: tube plugging. In order for the tubes to be effective, they must remain clear and in place. However, the incidence of occlusion has ranged from 1.4-36% [4-6, 9, 10]. Several treatments have been devised to address this problem from topical antibiotics and coatings to vasoconstrictors and tube composition.

Cunningham and Harley [6] used Polysporin ophthalmic ointment to determine if there was a difference in the incidence of postoperative hemorrhagic intraluminal obstruction. His findings show that the tubes without ointment were more likely to become obstructed with blood than the ointment covered tubes. However, these results were not significantly different. Altman et al. [5] proposed that the occlusions were the result of bleeding or effusion material during the surgical procedure. He used Phenylephrine hydrochloride, a vasoconstrictor, to prevent blood from occluding the tube. His results showed that the vasoconstrictor significantly reduced the incidence of obstruction and had little or no effect on the hearing of the patients. Tarek [3] performed a similar study on the effectiveness of vasoconstrictors in reducing occlusions postoperatively. The study used xylometazoline hydrochloride as the vasoconstrictor along with procedural changes during operation to determine their effectiveness. The results showed that after three months there were no cases of occlusion in the ears treated with the vasoconstrictor. In addition, a link between the diameter and length of the tubes demonstrated that shorter tubes with larger diameter were ideal for lowering the obstruction rate.

Consequent studies have been conducted to determine how geometry and composition play an important role in preventing long term adverse effects, such as permanent perforation of the ear drum. Apparently, the frequency of permanent perforation increases as a function of the tube length and diameter. Morris's [13] research showed that there is a relationship between geometry and permanent perforation of the tympanic membrane. Tubes with small diameters and lengths have only a 0.5%-3.4 % chance of perforating. However, the percentage increases to 8.5% using larger diameter tubes and long T-tubes have the greatest likelihood of perforation at 32.6%.

Furthermore, material composition may play a role in preventing occlusions. Silver oxide imbedded onto silicone tubes shows very good results. Other materials, such as ionized coated fluroplastic, thermoplastic elastomers, and titanium tubes also show promising results for reducing occlusions. Additional research on tube composition by Shone and Griffith [2] compared a titanium grommet tube to a Shepard grommet. The results showed that patients with the titanium tube had a large amount of granulated tissue covering the tube, whereas the Shepard had none. In addition, there was no significant difference in the duration of function between the tubes or that the more expensive titanium tube occluded less often than the Shepard. Saidi et al. [18] also discovered that the composition, specifically the adherence properties of the material, is extremely important in preventing occlusions. The study reported on the formation of bacterial biofilm on the surface of tympanostomy tubes manufactured out of various materials. Roland et al. [15, 16] performed similar studies of bacterial growth on vent tubes and possible topical solutions for relieving the resulting otitis media.

Studies were also performed by Arnold and Bressler and Westine et al. [4, 7, 20] to determine the effectiveness of various solvent solutions in clearing plugged tympansotomy tubes. Westine's experiments were performed in an ex-vivo chamber with the tubes plugged the night before with muccoid effusion. The ex-vivo chamber allowed for precise control of external variables and alleviateed the need for large patient studies. The results showed that common vinegar, hyaluronidase, and protease K were all statistically different from the control of water and cleared the tubes the fastest. Furthermore, research by Tsao et al. [19] showed that tube composition did not significantly affect tube clearance, but demonstrated potential as a possible catalyst for

plug removal. The research showed that smoother surface characteristics prevent bacterial adhesion, which is a possible cause of tube plugging. Additional studies performed by Mehta et al. [12] analyzed the effects inner diameter and shaft length have on the clearance of plugged tubes. The tests used ofloxacin otic solution, which is the only federally approved solution on the market to determine the effectiveness of various tubes. Once again the tubes were plugged the night before with muccoid effusion and then placed in a chamber. The time to clear was measured and the results showed that larger inner diameter tubes with longer lengths showed an accelerated rate of clearance. Despite these results, larger diameter tubes might allow more contamination of the middle ear, thus causing more mucoid effusion and more frequent tube obstruction.

Other research has proven that albumin is effective in preventing cell and protein adhesion Kinnari et al. [9-11] performed tests on albumin coated ventilation tubes to determine the change in surface texture of the tube. Albumin has been shown to prevent bleeding, and inhibit bacterial growth, fibrin adhesion, and thrombus formation. The results of his research showed that the bacteria were inhibited from growing on tubes coated with albumin. Additional research showed that there was less fibronectin adhered to the surface of the albumin coated tubes than those that were left uncoated. This is the direct result of albumins ability to produce a very smooth film over the coated surface of the tube. The smooth surface reduces the number of deep groves and pores in the tube, thereby decreasing the overall surface area and providing less space for adhesion of particles.

In-vitro Chamber

The use of in-vitro ear chambers to simulate biological conditions has been used in several of the above studies [4, 12, 19, 20]. These chambers eliminate complicated

biological variables and reduce the need for patient studies. Prior experiments did not test, however, for the formation of the occlusions. In fact, the tubes were forcibly plugged with mucus and allowed to dry without accounting for the method of occlusion. Also, there has been no research conducted on creating an in vitro model of the middle and outer ear to measure the real-time formation of the occlusions. This kind of device would reduce the need for patient studies and would allow accurate control of the variables within each experiment. In addition, the testing variables could be repeated under similar conditions to analyze tube performances. This chamber would specifically provide an environment that would mimic the middle and outer ear. Plus, the chamber would have inputs for mucus delivery, air, and will be driven with a load cell and syringe pump. The force and time could then be recorded as the fluid passes through the tube.

Mucus Analog

A component of this project is to find an analog to replace human mucoid effusions. A mucus analog is a fluid that has similar properties to the host fluid, but has additional advantages, such as cost, quantity, and safety. The majority of past studies have used human mucoid effusions to test the effectiveness of various tube types and plugging solutions. However, collecting human mucoid effusions is time consuming and expensive. In addition, in order to obtain the quantities needed for experimentation, samples from each patient must be pooled together as one. The resulting effusion also poses a health hazard to the researcher, since many of the samples contain blood and other pathogens. In addition, one pooled sample may differ from another pooled sample in viscosity and composition. Nevertheless, despite these disadvantages, the conclusions drawn from the results can be used to determine how the tubes will behave in an in-vivo environment.

Mucous analogs, such as egg yolk and egg white, have the advantage in an experimental atmosphere because they are cheap and can be easily obtained. Egg yolk has an average viscosity value of 900 cp. Yolk also poses no immediate health risks to the researcher. Furthermore, relatively large quantities can be obtained from just one egg, allowing for numerous experiments to be performed. Egg white also poses no immediate health risks and has an average viscosity of 100 cp. In addition, egg white is mostly composed of albumin which is one of the components of blood. Also the physical characteristics of egg white is similar to human mucus in that it is "chunky" and does not form uniform droplets when squeezed through a syringe. However, to reduce the number of variables caused by the random "chunks" in egg white, egg yolk with its more consistent viscosity and physical characteristics will be used. The only drawback of mucus analogs is that the outcomes can not be used to ascertain a direct relationship between laboratory and in-vivo environments.

In short, it is critical to understand the mechanisms which cause occlusions. The goal of this research, therefore, is designed to shed light on the causes of this occluding and to develop a device to examine variables which would be impossible to analyze using patient studies. While previous research has always been conducted post-plugging, this research will be performed in real time with the occlusion rate monitored as the tubes plug. The present research will use a mucus analog (egg yolk) which has similar mechanical, behavioral, and physical properties as human mucus but is available in large quantities and is relatively safe to use. The results of this research will be used to validate the ability of the flow system to detect both the formation and removal of occlusions as they occur.

CHAPTER 3
MATERIALS AND METHODS

Chamber Design

Ear Flow Chamber Overview

The ear flow chamber was designed to allow a fluid to flow through a tympanostomy tube. Figure 3-1 shows a schematic overview of the flow mechanism. The basic principle of operation is that a fluid is pushed towards the input of the chamber. The force required to push the fluid through the tube is measured using a load cell. Air is occasionally pumped into the chamber in front of the tympanostomy tube to simulate the natural opening and closing of the Eustachian tube. The air also aids in the drying of the mucus. The ear chamber holds the tympanic membrane and tympanostomy tube in place during operation. Finally, the tympanostomy tube is where the mucus exits and eventually dries, forming an occlusion. This occlusion causes the pressure within the chamber to build up, causing the force required to move the fluid through the tube to increase. The force is subsequently measured and the occlusion time can be determined.

Membrane Design

A tympanic membrane was designed to mimic an in-vivo tympanic membrane. This design provided a repeatable method for manufacturing a holding mechanism for the vent tube as well as mimicking the surgical technique used in the medical field.

During the surgical procedure, a small incision is made in the tympanic membrane and a vent tube is inserted. After one day, the body naturally heals the incision around the tube and holds it in place.

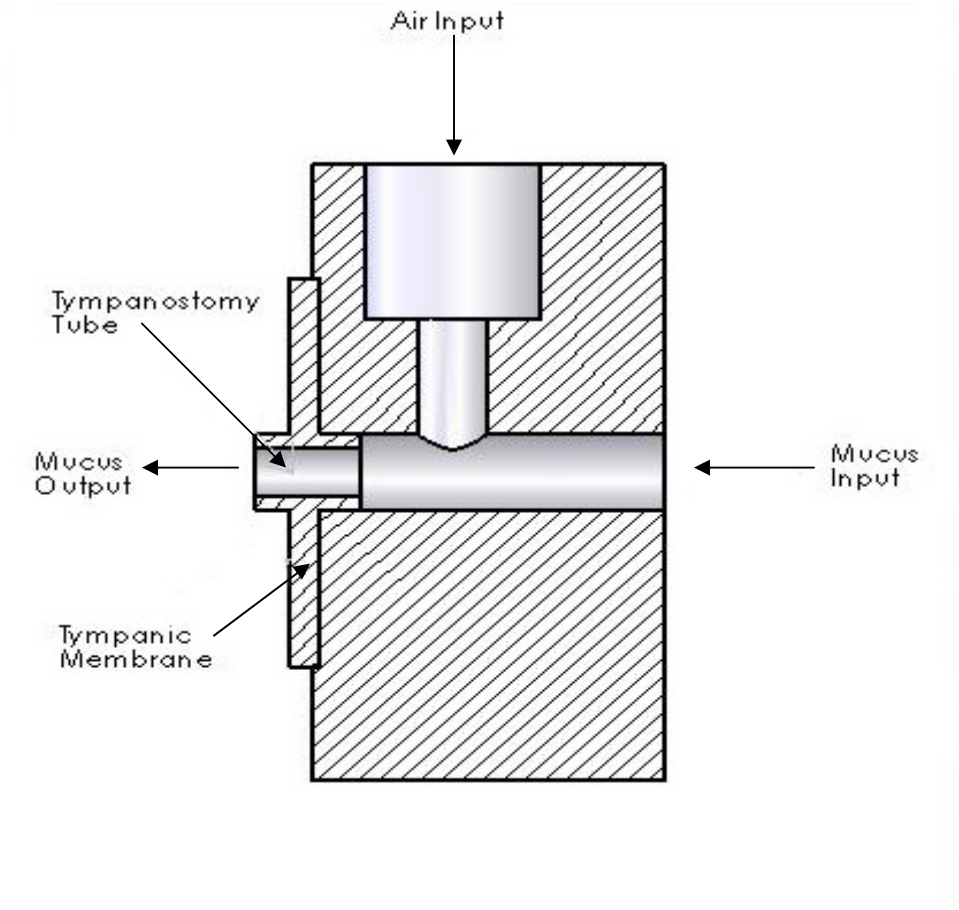

Figure 3-1: Schematic overview of the ear flow chamber.

Likewise, an artificial membrane was designed to support a vent tube and keep it securely in place. The artificial tympanic membrane was made with a rigid metal washer (Steel, 0.625 inches outer diameter, 0.50 inches inner diameter, 0.01 inches thick) supporting a thin elastic membrane across it (Microflex, Diamond grip, Power free latex exam gloves). The elastic membrane was attached to the metal ring using a spray adhesive (Elmer's Craft Bond, Multi Purpose Spray). The elastic membrane has properties that allow it to conform, holding the vent tube in position. In addition, the ring has properties that allow it to maintain its shape as the membrane deforms. Furthermore, since the ring was circular, it can distribute the pressure force evenly over the entire surface of the membrane.

Additionally, this latex membrane was chosen because of its elastic properties. The latex tends to conform around a hole forming a tight seal (Figure 3-2). Therefore, if the latex is punctured with a small slit in the relaxed state (1), in the stretched state the hold will be large enough to fit the tube (2), and then after the tube is inserted the relaxed latex will conform around the vent tube and hold it in position (3). However, in most cases where the vent tube is smooth, a small amount of super glue was used to hold the tube in place and prevent leaking during experimentation.

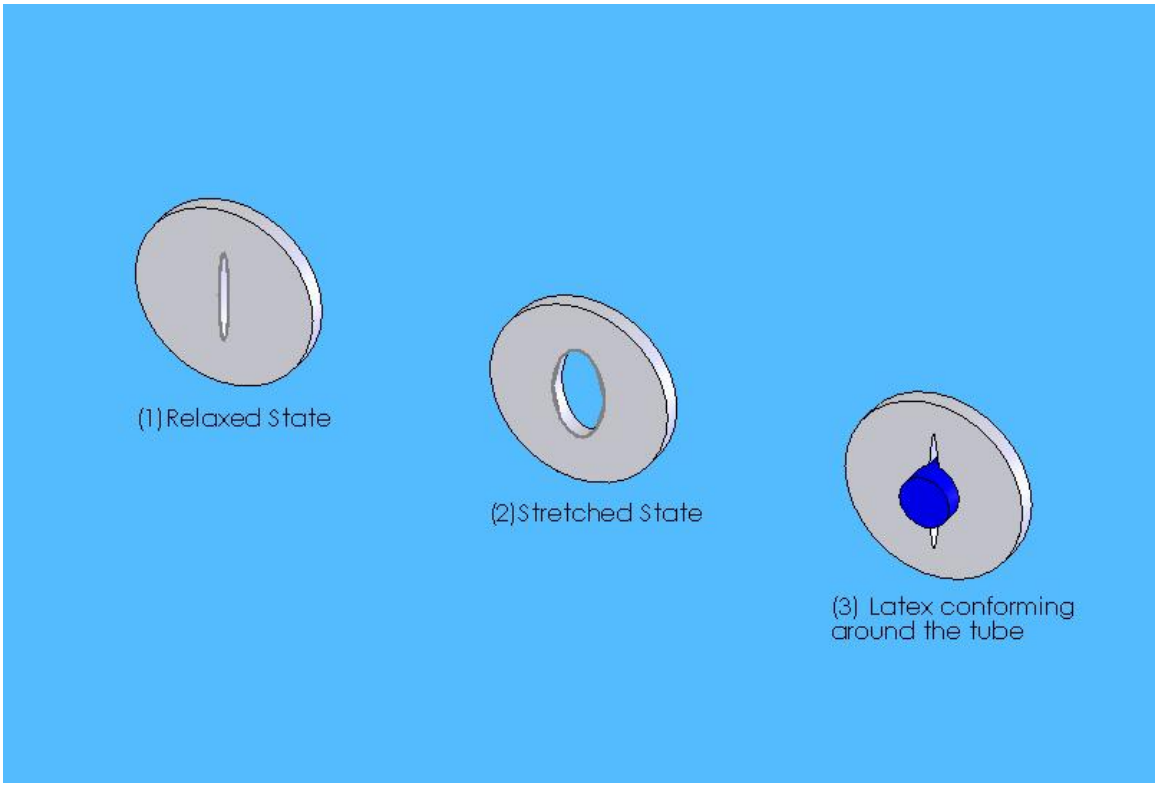

Figure 3-2: Progression of latex membrane during setup.

Chamber Geometry

To test the vent tubes, a chamber was built out of Lexan plastic to mimic the environment within the ear canal (Figure 3-3). The ear consists of the external (outer) ear, middle ear, and inner ear. This chamber reproduces both the outer and middle ear

environments. In addition, there are three primary functions of the chamber. The first function was to hold the vent tube (C) and membrane (E) in place throughout the experiment. The membrane is held in place by a circular indentation in the chamber. The membrane was held against the front of the channel by a foam seal (B) and Lexan compression plate (A). The foam seal was designed to prevent air from leaking out of the front of the chamber as the pressure builds up. The Lexan compression plate squeezes the membrane and foam seal by using four machine screws. The compression plate also has a hole in the center to allow the mucus to drain out of the tube. The second function was to provide a port for the mucus to be delivered (F). In the center of the chamber about half way between the front and back is a port that connects to an air filled syringe (G). All of the attachments are made with "Luer" lock connections, which allows for easy assembly.

Load Cell

The force required to depress the fluid filled plunger was measured and recorded throughout the experiment in order to gauge the effectiveness of the tympanostomy tubes. As the fluid passes through the tubes, a small amount of it accumulates at the entrance, exit, and inner surface of the tube. Over time, as the tubes become occluded, the force required to depress the plunger increases, which can be documented with a computer. The force reading was obtained using a load cell (Transducer Techinques, SB0-50, 165994) (Figure 3-4). The load cell measures force by calculating the change in resistance of a strain gauge as the metal it was attached to deforms. The resistance was detected using a Wheatstone bridge circuit (Figure 3-5). This circuit was connected to an operational amplifier which increases the output voltage (gain) of the signal from mili-volts to volts.

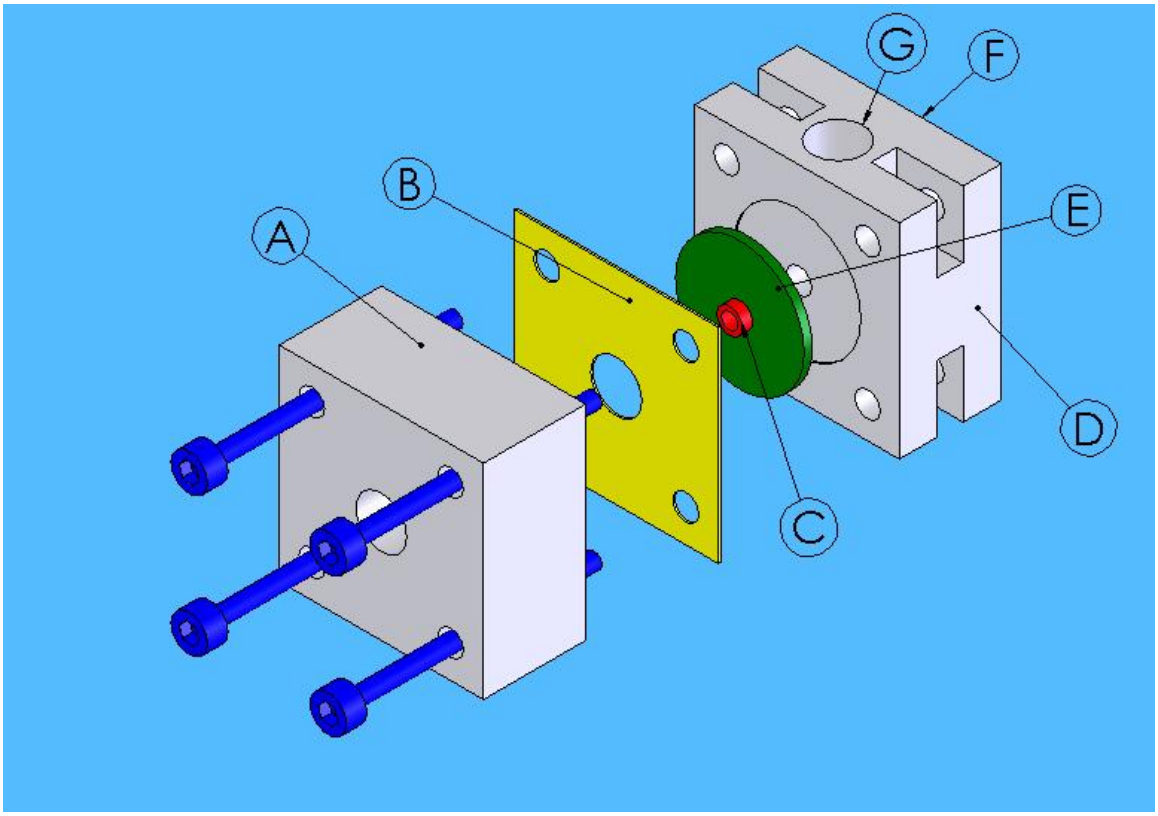

Figure 3-3: Exploded view of the ear chamber. (A) Front compression plate. (B) Foam seal. (C) Vent tube. (D) Ear chamber. (E) Latex membrane with ring. (F) Input for mucus. (G) Input for air.

Figure 3-4: Load cell.

A Wheatstone bridge circuit is composed of two voltage dividers fed by the same input. The output was connected to a galvanometer (a very sensitive DC current meter), which measures the current flowing from each of the voltage dividers. If the output is

balanced (R1/R2=R3/R4), then the circuit has no current flowing through it. However, if one of the resistors is changed by a small amount, then the galvanometer becomes a very accurate indicator of the balance of the circuit.

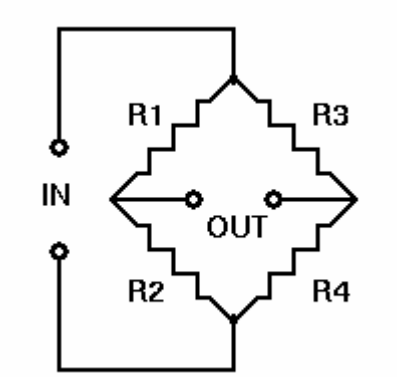

Figure 3-5: Whetstone bridge circuit.

Operational Amplifier

An operational amplifier (op-amp) circuit (Figure 3-6, 3-7) was used to boost the voltage of the load cell signal so that it can be measured using the DAQ board and Labview program. The amplifier was designed to be non-inverting and consists of a LM741 microchip, 10K potentiometer, and resistor. The gain of the amplifier was determined by dividing R2 (562,000Ω resistor) by R1 (5,300Ω resistor). In this case, the gain was 106.04. The positive signal was fed into the op-amp and the amplified output was connected to the DAQ board along with the negative portion of the signal.

Circuit Design

DAQ Board

A Data Acquisition Board (DAQ) (Measurement Computing, Middleboro MA, PMD 1208FS) is a device that can both control external devices as well as acquire data from many different sources using a computer (Figure 3-8).

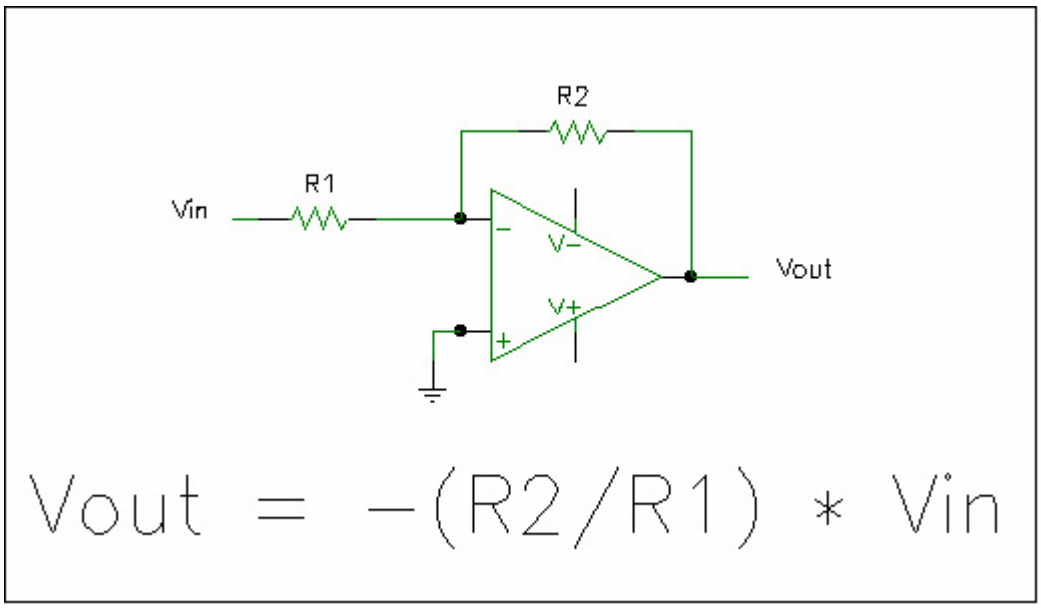

Figure 3-6: Schematic of 741 operational amplifier.

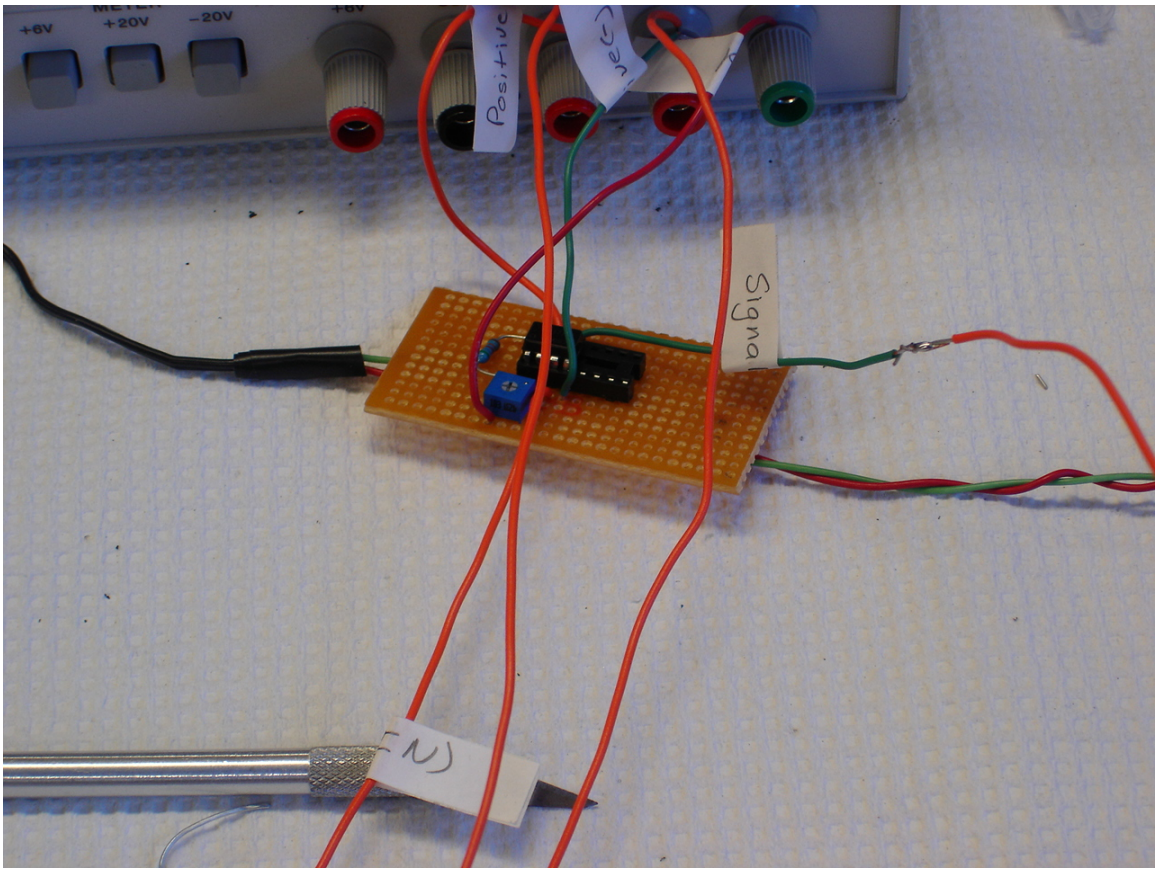

Figure 3-7: Operational amplifier circuit.

The DAQ board has several analog inputs and two independent analog outputs, each of which has a maximum output voltage of 4.1V and 15mA. For this project, the voltage signal was acquired and the air flow and mucus delivery are all controlled using the DAQ board. This device was connected to the computer via a USB (Universal Serial Bus) port. During setup, the first of the analog outputs (Channels 12 and 13) were used to control a 12V DC motor and the second (Channels 14 and 15) were used to control the 120V AC power source running the syringe pump, load cell, and operational amplifier. However, since the voltage of each of the output devices exceeds the output voltage of the DAQ board, an additional circuit was built to control the two devices.

Figure 3-8: DAQ board with input and output connections.

Voltage Concerns

One of the main concerns of this project was the limited power source provided by the DAQ to control high voltage devices. The problem was initially discovered when

the need to control the rate of mucus and air over long periods of time became important. A solution was devised using the existing DAQ board with its computer controls along with an additional circuit that will control the high voltage external components.

The design of the circuit was dictated by the use of transistors and relays which are electrical components designed to handle the task of controlling high voltage devices using low voltage sources. In this case, the 10V DC current driving the syringe pump would damage the delicate circuitry of the DAQ board if connected directly. However, through a relay switch, the voltage can be safely turned on and off with as little as 9V DC. The same applies to the gear head motor, which requires at least 9V DC to run. The output of the DAQ board was only 4.1V so an external 9V power source was connected to the circuit and controlled with a relay. Below is a detailed description of the components within this system.

Optical Circuit Design

The electronic circuit serves as a middleman between the DAQ and output devices. This circuit was designed using an optical switch. The switch was intended to take advantage of the properties of a NPN transistor, allowing a low voltage to drive a much higher voltage. The NPN transistor (Figure 3-9) operates as follows: "C" is the collector, "B" is the base and "E" is the emitter. When a high voltage electric current was applied across E and C and a low voltage was applied at B, then B acts as a switch allowing the high current to flow from E to C. Therefore, if there was no voltage applied at B, then low current will flow. Conversely, when a voltage was applied at B, then the high current flows through. Harnessing this principal, the circuit was designed using optical sensors and high voltage relay switches.

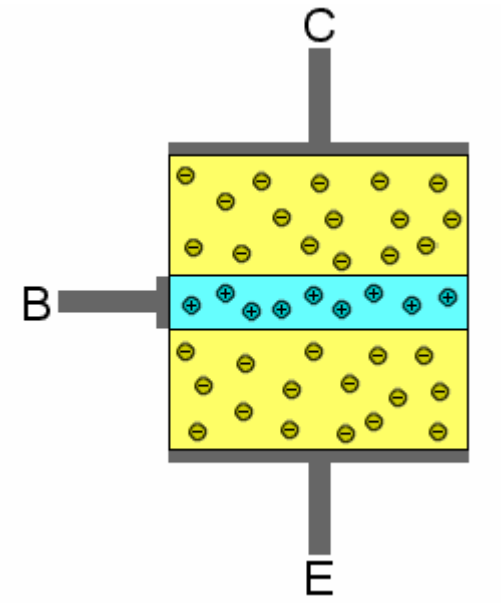

Figure 3-9: Schematic diagram of an NPN transistor.

A relay switch was used to control the high voltage sources needed to operate the output devices. These output devices include a 12V gear head motor (Jameco, GH12-1632TL, 69 RPM) and an electrical outlet. A relay is an electromagnetic switch that uses a low voltage electromagnet to control a lever between two different terminals (Figure 3-10). This relay along with a 10KΩ potentiometer (Jameco, ½ Watt trimming pot, 3362P1), a transistor (2N3904, NPN, 100mA), a bright white LED (Light Emitting Diode) (Jameco, TFUW83C, 3700mcd), and a photocell (Jameco, CDST05, 10KΩ-100KΩ) make up the components of the circuit.

Figure 3-11 shows the schematic wiring diagram of the entire circuit including both optical switches and the printed circuit board. The circuit works as follows. First, the 4.1V supply was turned on by the computer which lights the white LED. The photocell detects the change from dark to light and modifies its resistance. A high voltage (9V) current passes through the photocell and into the base of the transistor as well as the potentiometer.

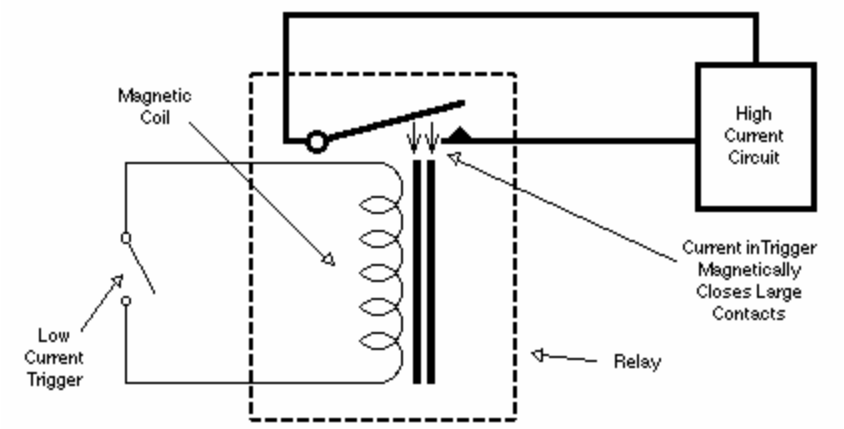

Figure 3-10: Schematic diagram of a relay switch.

The emitter end of the transistor is connected to the high voltage (9V) source and the collector is attached to the lever arm of the relay. Therefore, as the LED is turned on and off, the resistance changes within the circuit and the relay flips up or down turning the motor on and off. The second relay switch works in a similar manner. However, it controls the voltage supplied to an electrical outlet. As the LED is turned on and off, the relay switch turns on / off the syringe pump, load cell, and op-amp. Figure 3-12 shows the optical circuit board held within its plastic enclosure.

Labview Design

Data Acquisition

One of the goals of this project was to accurately measure the change in force applied to the syringe over time as the vent tube occludes. This was achieved using a DAQ board and a computer program called Labview 7.0i (National Instruments Corp. Austin TX). Labview is a programming language used to control devices and acquire information from external electrical components. In this case, Labview needs to collect the voltage signal as well as control the rate of air flow into the chamber.

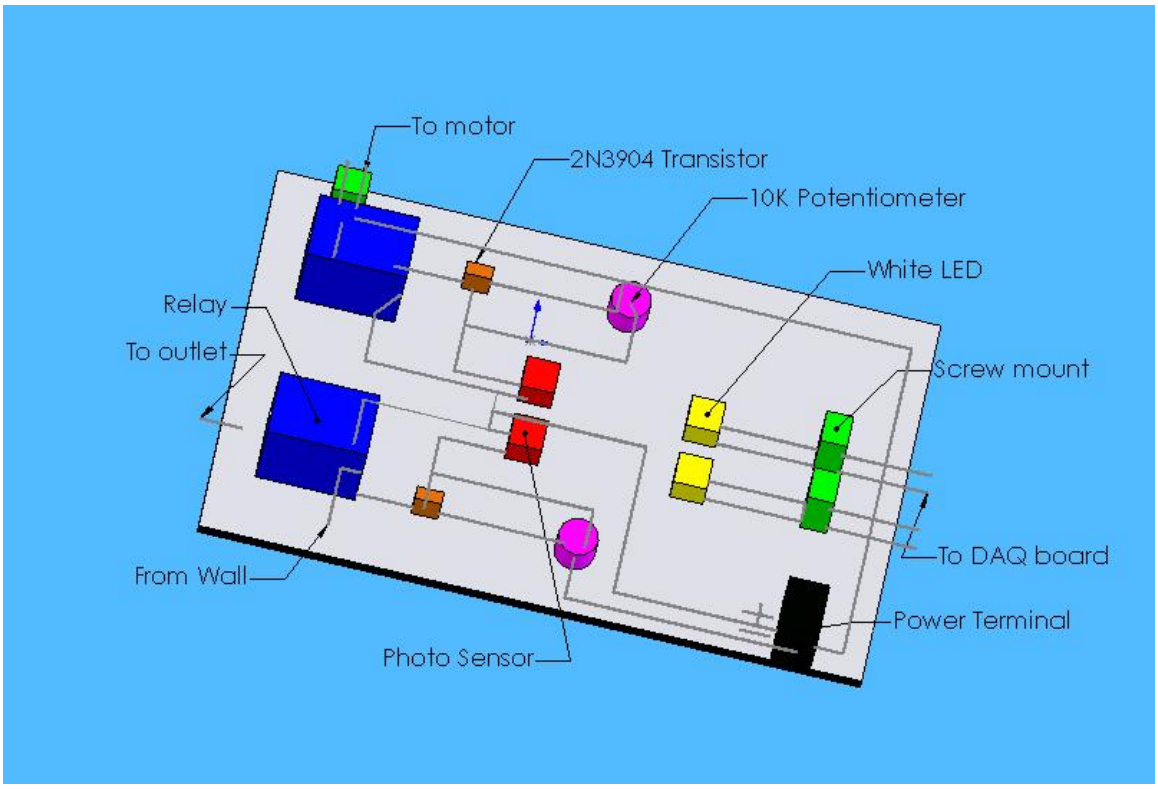

Figure 3-11: Schematic diagram of the optical relay circuit.

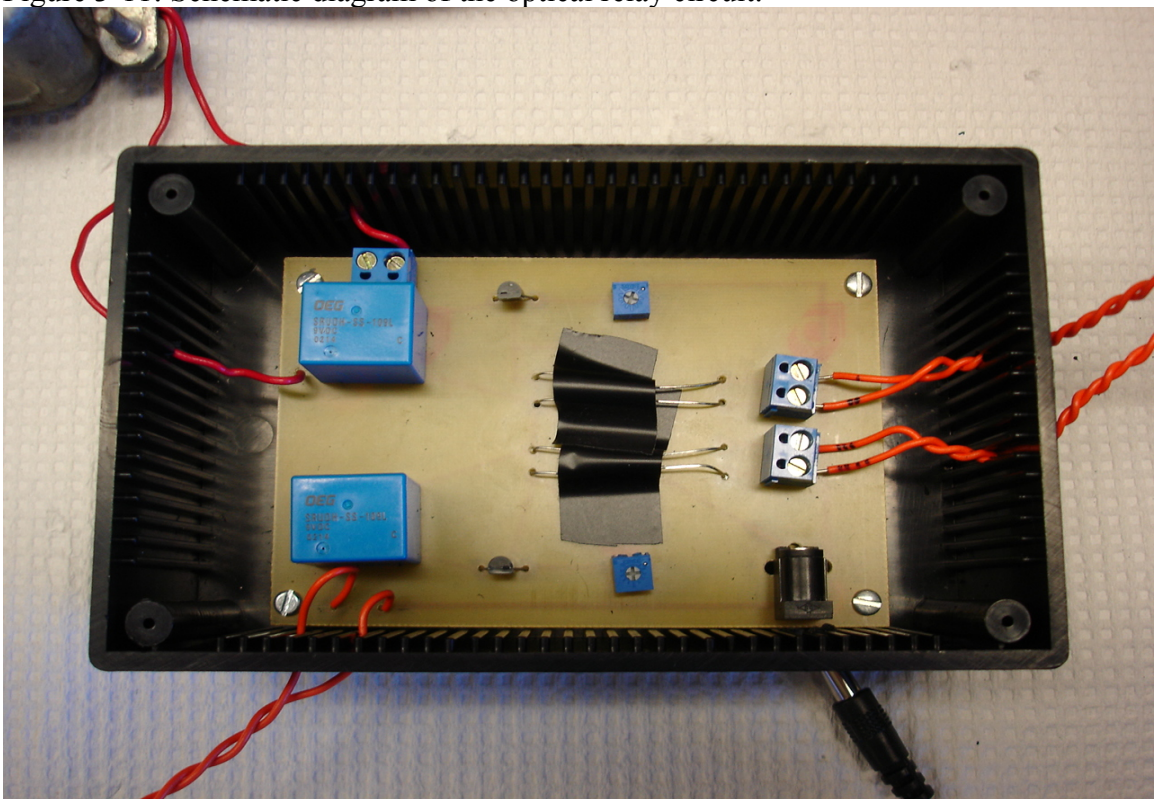

Figure 3-12: Optical circuit in housing.

For this project, the Labview program was written to run for 2 hours or until a maximum allowable rate was achieved (slope = ~8.33). After that, the program automatically turns off the syringe pump, load cell, and operational amplifier and saves the force and time data. Plus, the force and time data was sampled at a rate of 0.4 Hz. Therefore, over 2 hours there will be a total of ~1,800 data points which, when analyzed with Excel, will not exceed its limit.

Another unique function of the Labview program was that it was easy to accommodate a change in protocol. In other words, multiple users can perform the experiment with little or no programming knowledge. See Appendix A for a detailed schematic of the program.

Motor Control

The computer program functions to control the duration and frequency of air droplets into the chamber. This was achieved by using the electric motor and Labview. The resulting drops are determined by the distance traveled by the plunger as the motor turns. As a result, a relationship can be made between rotational time and syringe volume. Therefore, the Labview program can deliver an air drop of 0.05ml every 5 minutes. See Appendix A for a more detailed look at the program.

Syringe Pump Design

Syringe Scaffolding for Air Flow

A self contained aluminum scaffold was used to hold the entire drive mechanism for delivering air and provides a location for attaching the ear chamber (Figure 3-13). The scaffold consists of two plates (C & E) attached to a base plate. The bottom plate is fixed to the base, whereas the middle plate is attached to a threaded rod (D) and is free to move up and down as the rod turns. The middle plate contains a series of small clamps

that secure the movable end of the plunger, while clamps on the bottom plate secure the barrel of the syringe. Therefore, as the middle plate moves, it depresses the plunger and delivers the volume of air. At the top end of the scaffolding, there is a motor (F) attached to the threaded rod which provides the rotation.

This entire scaffolding mechanism was attached to a large "L" shaped base (A) which holds the syringe scaffolding in the vertical direction. This base has a large hole cut out towards the bottom end (B), which allows the fluid filled syringe to attach to the chamber.

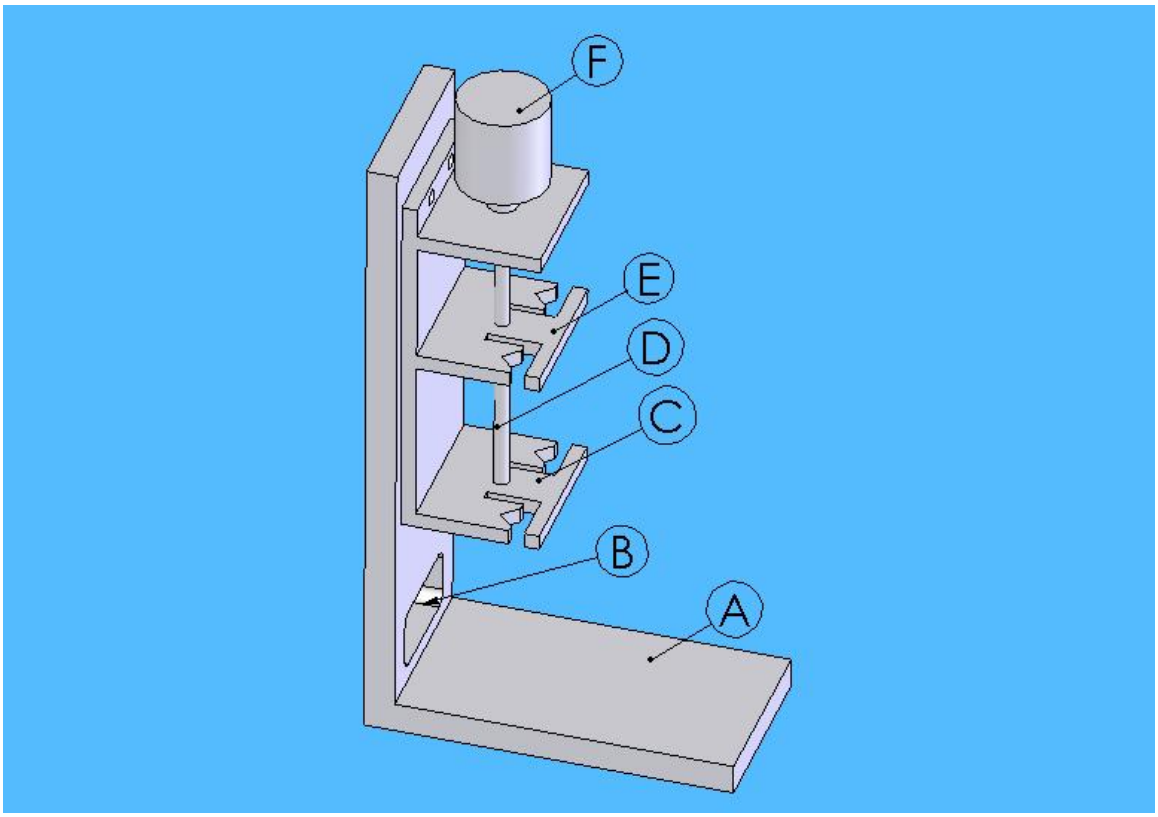

Figure 3-13: Detail of syringe scaffolding with motor. (A) base. (B) pass-through for air flow. (C) syringe holder. (D) threaded shaft. (E) moving plunger depressor. (F) gear-head motor.

Motor Drive for Air Flow

In order to administer the air in a controlled manner, a 12V gear head motor was used (Jameco, GH12-1632TI, 11kg/cm). This motor was chosen because it has a high starting torque of 11KG/cm and a low speed of 69 RPM (revolutions per minute). However, the motor provides a rotational motion which must be converted into a linear motion to depress a plunger. This mechanism was known as a screw drive. A screw drive mechanism was composed of a long threaded rod which is attached to the shaft end of the motor. This threaded rod has a known thread count and is fixed at both ends. A plate with a threaded hole in the center can then be attached to the rod. As the rod rotates, the plate can travel linearly along the length of the shaft. This movement can be precisely controlled by the duration of rotation and number of threads per inch on the rod. Therefore, the rotational motion of the motor can be applied in a linear manner (Figure 3-14).

Syringe Scaffolding for Fluid Delivery

The flow of fluid (mucus) within the syringe was controlled using a custom made syringe pump (Figure 3-15). The scaffolding consists of three fixed aluminum plates held between four aluminum rods (D). A stepper motor (H) was attached to the central plate and a long threaded rod (G) was attached to its shaft. This shaft was threaded through an aluminum rod (E), which was attached to a key (F). The key consists of a small “L” shaped piece of aluminum. When attached to the threaded aluminum rod, it prevents the rod from rotating, but allows it to translate. The other end of the aluminum rod was attached to one end of the load cell (C), while the other end of the load cell was attached to the plunger on a syringe (B).

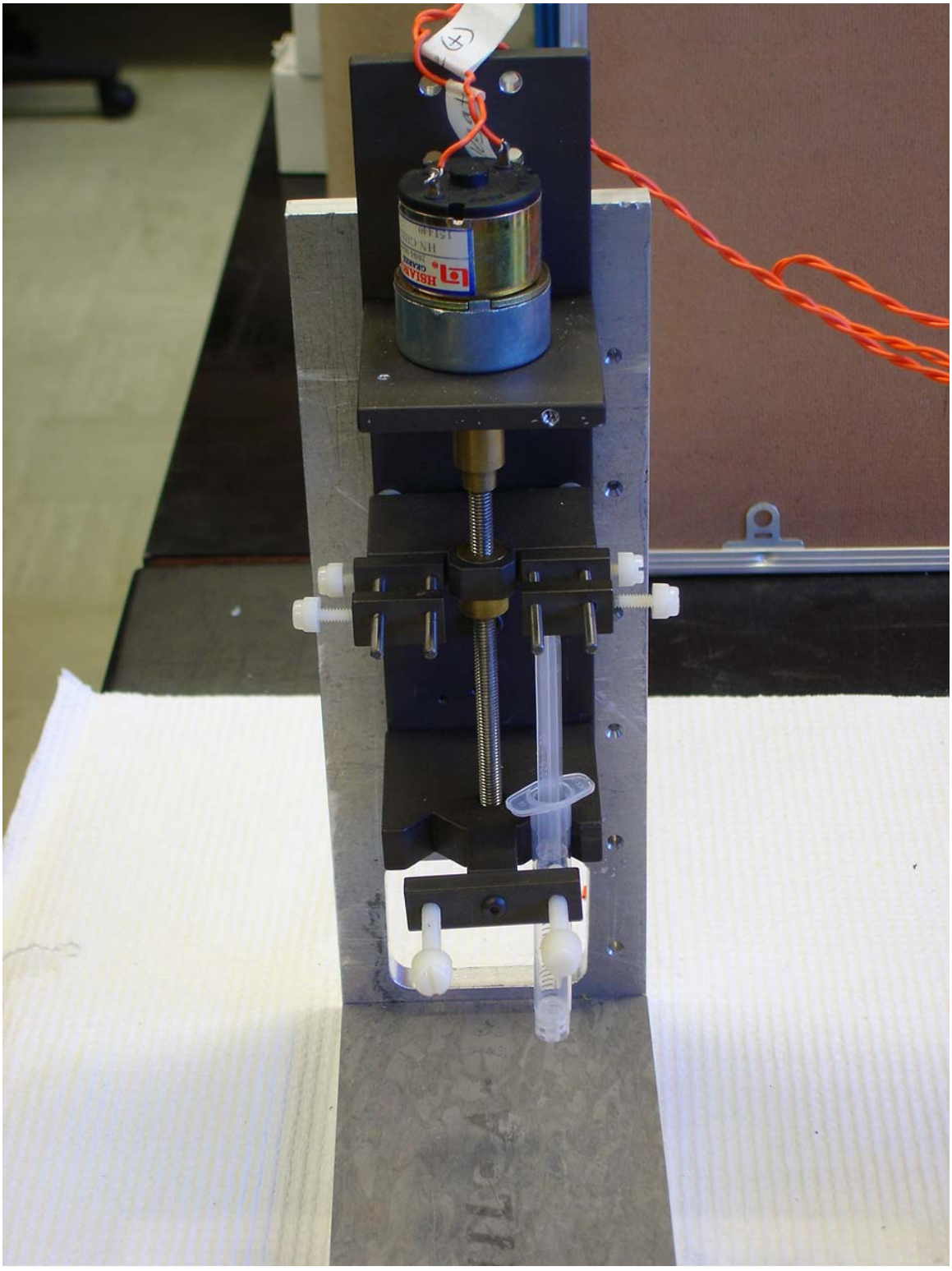

Figure 3-14: Motor mounted on syringe pump and scaffolding.

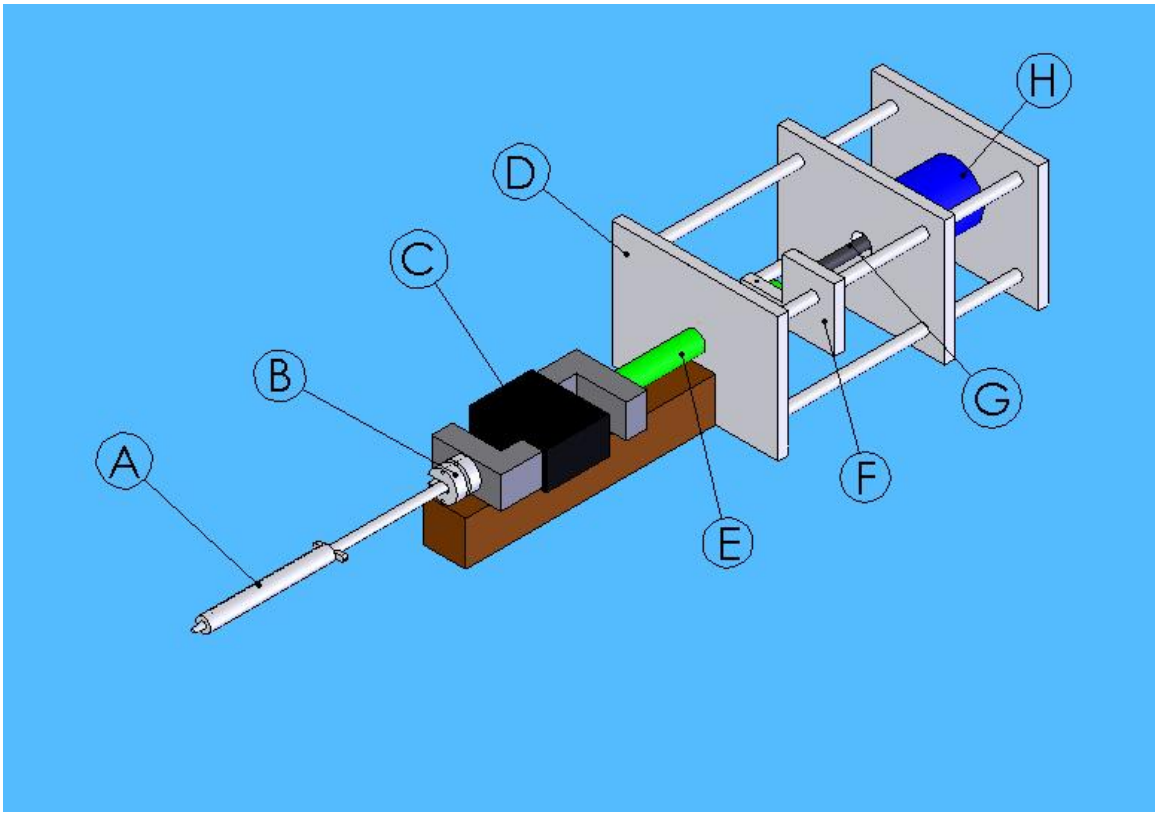

Figure 3-15: Syringe scaffolding for fluid delivery. (A) Syringe. (B) Syringe plunger holder. (C) Load cell. (D) Aluminum scaffolding. (E) Aluminum rod. (F) Key. (G) Threaded rod. (H) Stepper motor.

Motor Control for Fluid Delivery

The stepper motor was controlled using a stepper motor driver kit (Jameco, Diy Kit 109 Stepper Motor, 139109). The driver was designed to control a 5 lead unipolar stepper motor. The circuit controls direction, step rate, full or half steps, and speed. In addition, the circuit can be computer controlled for easy adjustments. Figure 3-16 shows the schematic diagram of the circuit.

Additional modifications were made to the circuit board, including rewiring the switches so that they can be mounted on the outside of the box. Plus, after several test runs, the flow rate of the factory circuit was faster than the flow rate required for

experimentation. Therefore, an additional 1.5MΩ resistor was added to the potentiometer to slow the step rate of the motor.

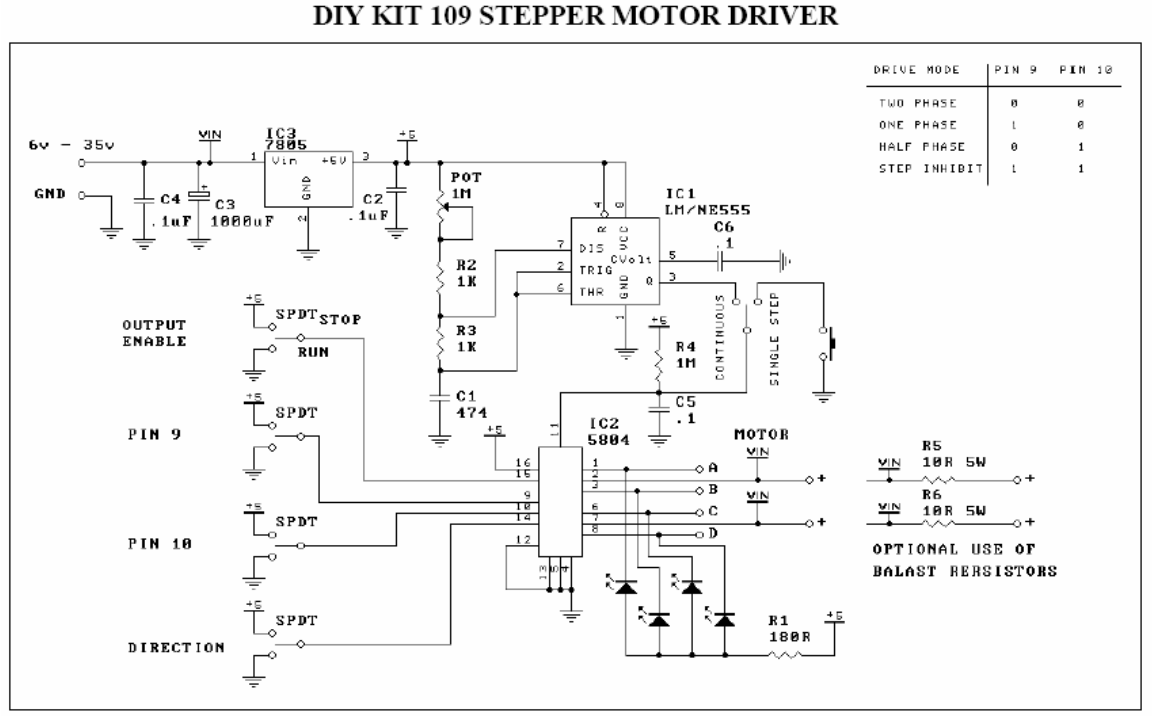

Figure 3-16: Unipolar stepper motor driver schematic.

Experimental Setup

Testing Procedure

The following procedures describe the step by step processes for each experiment. The first objective was to create the tympanic membrane. A metal washer (0.625 inches outer diameter, 0.50 inches inner diameter, 0.01 inches thick) was placed on a paper towel and a thin coat of spray adhesive (Elmer's Craft Bond, Multi Purpose Spray) was applied to one side of the washer. The glue was then allowed to dry for 5 minutes or until sticky, but dry to the touch. The next step was to cut a one inch by one inch latex square from a standard latex glove (Microflex, Diamond grip, Power free latex exam gloves). The latex square was pressed firmly onto the glued surface of the washer and pulled taut,

to eliminate dimples and folds on the surface. Most of the excess latex was cut from around the outer edge of the washer, leaving a small amount for future readjustment. Finally, a small incision 0.3125 inches from the outer diameter of the washer was made using a sharp pointed razor blade. The incision should be made approximately 1-2 mm in length. Once the above steps are completed the desired tympanostomy tube can be inserted into the artificial tympanic membrane.

When inserting bobbin shaped tubes, a pair of curved pointed tweezers was selected. One arm of the tweezers was placed into the canal of the tube and the other along the outer surface of the tube. The outer flange of the tube was then wedged into the hole of the latex, with the uncovered face of the washer facing the tweezers. The tweezers are gently removed while retaining the tube in the latex. Finally, the excess latex on the outer edge was used to readjust the membrane until it was taut. The remaining latex was cut off with a scissor. The last step was to apply a small amount of super glue (Lil Auto Store, LA-037, Iowa) to the slit in order to seal the tube in place and prevent leaking.

The procedure was slightly different for tympanostomy tubes that are “T” shaped and have a smooth body. A curved pointed set of tweezers was selected. Approximately 2-3mm of each of the ends of the “T” was trimmed in order to fit the tube in the chamber. Then the “T” shaped flanges of the tube are squeezed between the ends of the tweezers and the tube was orientated so the entire length lies between the ends of the tweezers. Next, the tweezer/tube device was inserted into the incision in the latex, with the uncovered face of the washer facing the tweezers. The tweezer was gently removed from the membrane leaving the tube secured within the incision. Following this, the tube was

adjusted so that the “T” shaped flanges are resting slightly above the membrane surface. Finally, the latex was readjusted until taut and any excess latex was cut from the outer edge of the washers as needed. A small amount of super glue was applied to the slit to prevent leaking and to secure the tube in place. Figure 3-17 shows some common “T” shaped tympanostomy tubes.

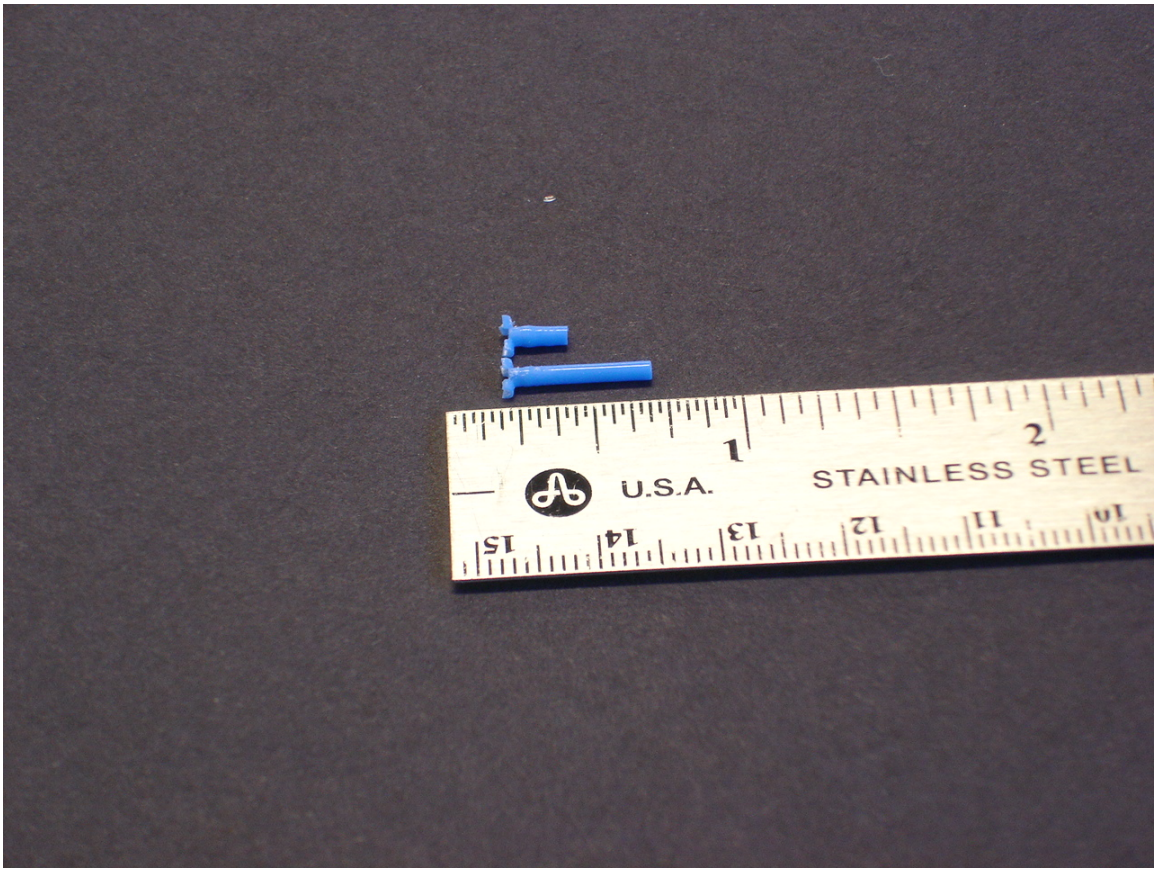

Figure 3-17: "T" shaped vent tubes.

Once the artificial tympanic membrane was complete, the foam seal can be made. A foam square (Darice Foameies Sheets, 2mm thick) was cut to the dimensions of the front face of the ear chamber. Then four holes are created with a hole-puncher corresponding to each of the four screws. An additional hole was cut with a hole-puncher that corresponds to the canal of the artificial ear chamber.

A small amount of vacuum grease (Dow Corning, High Vacuum Grease, USA) was now applied to the front face of the chamber and then the tympanic membrane was placed into the recess of the chamber, with the uncovered edge of the washer facing out. Next, the tympanic membrane was aligned with the flow port of the chamber so that the bottom of the tube was resting as close to the bottom of the chamber as possible. The foam seal was placed over the tympanic membrane with the five holes carefully aligned with the chamber. While holding the seal in place, the compression plate was placed over the foam and the holes in the compression plate are aligned with the chamber. Next, all four nuts are placed into the slot in the chamber and a screw (0.136 inches diameter, 1 inch long) was pressed through the plates and threaded through the nut. All of the four screws are then securely tightened with an Allen wrench. Figure 3-18 shows the assembled chamber.

Once the above steps are complete, the chamber was taken over to the syringe scaffolding where a 1 ml syringe was filled with mucus (yolk). The 1 ml syringe was attached to the load cell by threading the plunger attachment to the load cell. The mucus syringe was then attached to the input of the chamber via a Luer lock connection. The air flow syringe was connected to the middle of the chamber and the syringe was secured within the scaffolding and tightened down. Figure 3-19 shows the syringe setup.

Then the computer was turned on and the DAQ board was plugged into the USB port. The data acquisition Labview program was opened and the save file was changed to represent the test being performed. The power supplies were then plugged into the controllable outlet.

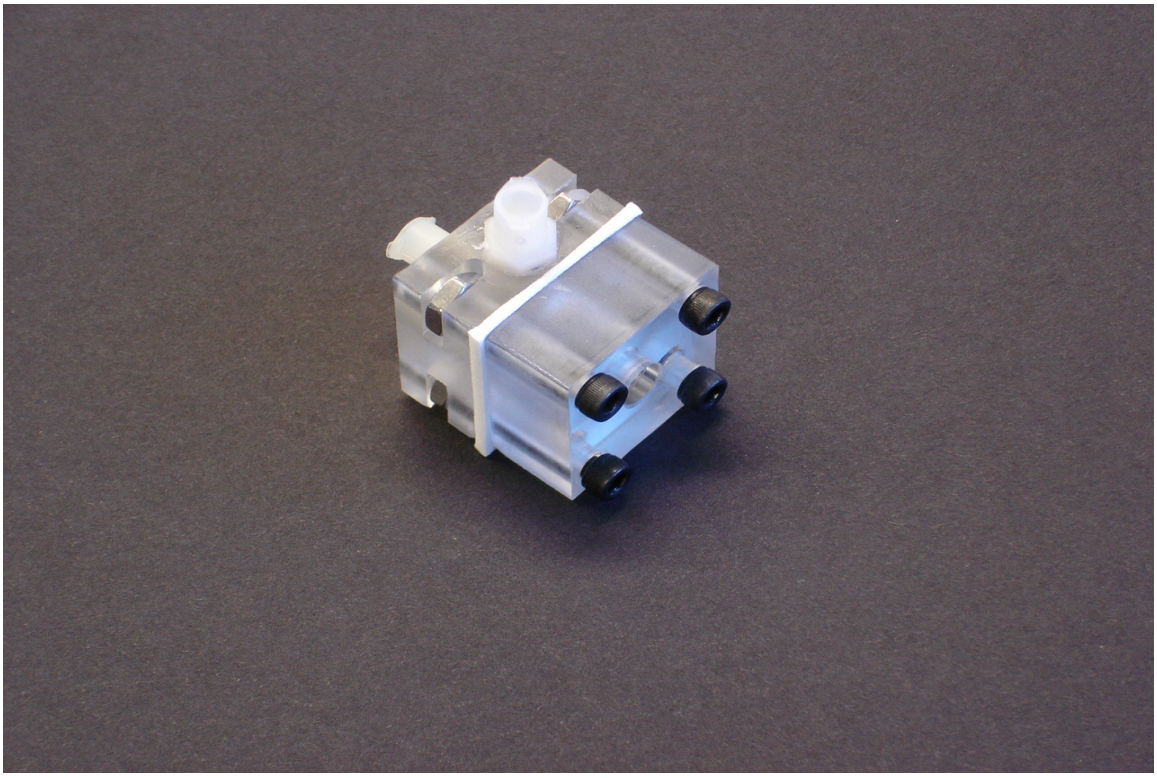

Figure 3-18: Assembled ear chamber.

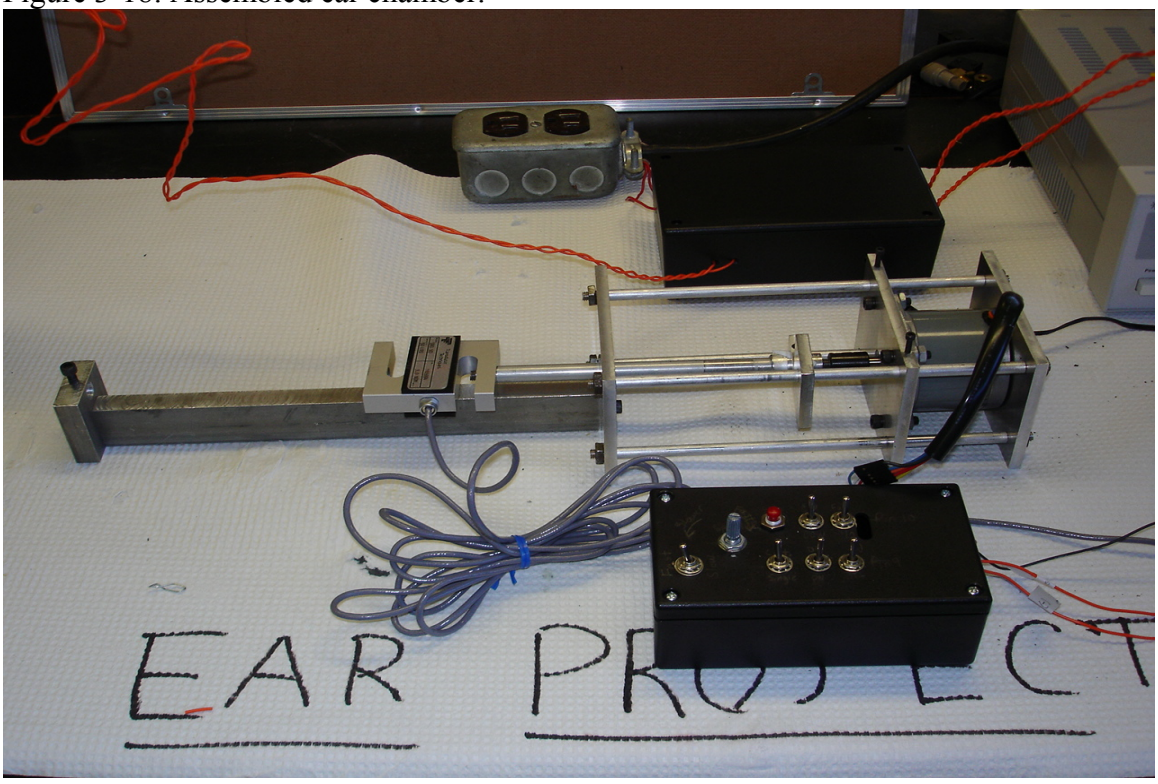

Figure 3-19: Ear chamber setup with load cell and stepper motor control box.

The pre-filling procedure was conducted until 0.10-0.15ml of fluid was in the chamber and a small amount of fluid had exited the tube. Then, the data acquisition Labview program was executed. The black box turned on the power supplies and the stepper motor control box rotated the screw and delivered the fluid through the tympanostomy tube.

Experimental Conditions

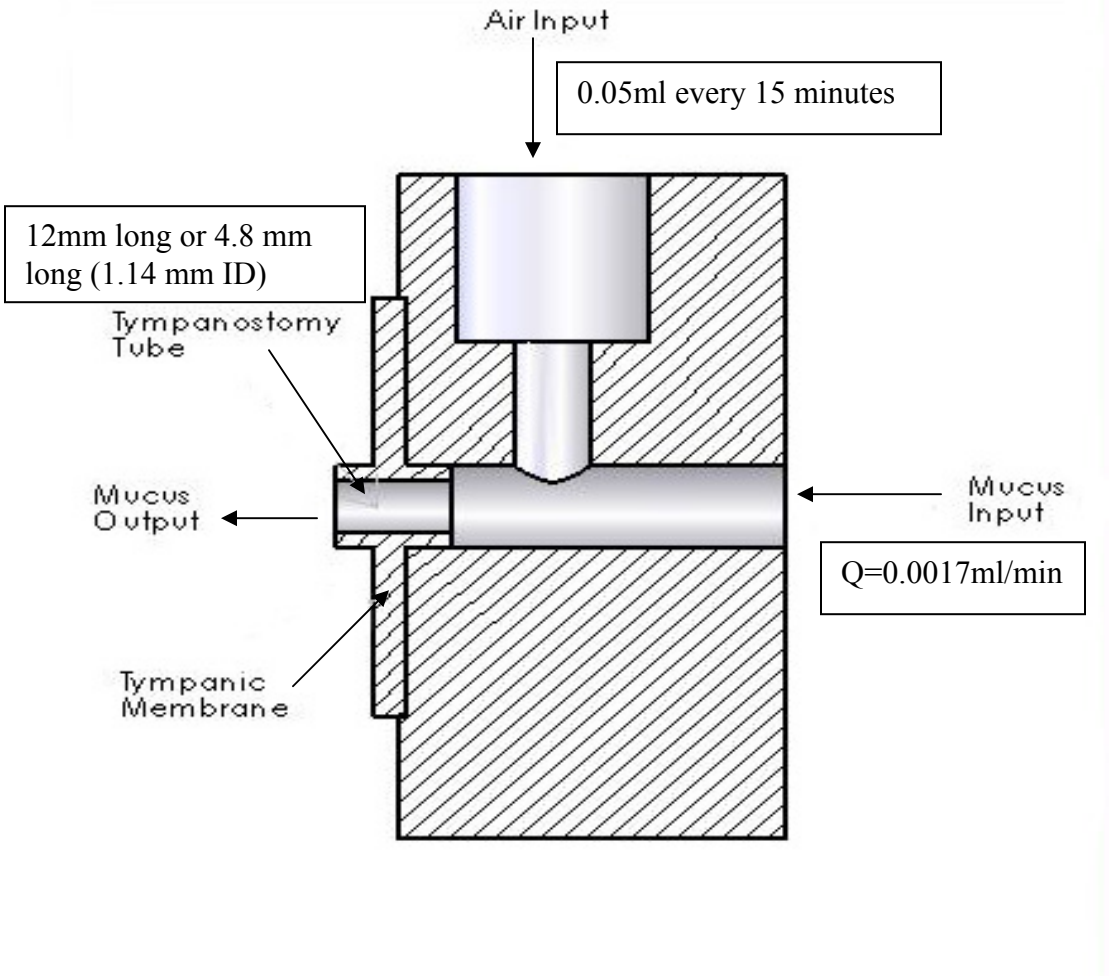

Figure 3-20: Experimental conditions.

Figure 3-20 shows the experimental conditions used for each test run. The environment consisted of a constant mucus flow rate (Q) of 0.0017 ml/min. Then air was input into the chamber every 15 minutes at a volume of 0.05ml. The tympanostomy

tubes were varied between 12mm and 4.8mm long and they both had an inner diameter of 1.14mm. Finally, throughout each experiment the force required to push the mucus through the tube was recorded.

CHAPTER 4
MEASUREMENT AND CALIBRATION

Viscosity of Egg Yolk

The viscosity of the egg yolk used as the mucus in this project was obtained using a Brookfield Cone and Plate Viscometer (Brookfield Engineering Laboratories Inc., Model: RVTDCP, S/N A03976). See Appendix B for the theory of operation of the cone and plate viscometer. The viscometer was calibrated following the instructions listed in the operating manual prior to testing samples. Once calibrated, a 0.5ml sample of egg yolk (egg white was tested as well) was placed into the chamber and a reading was obtained. The speed (RPM) of the viscometer was set to either 1 or 10. This experiment was performed 4 times to account for variability in the results. In addition, samples from several different eggs were tested in a similar manner to determine if there was any significant difference between the samples.

The average viscosity was then calculated after collecting samples from several eggs. The viscosity was 799.78 centipoises for the egg yolk and 103.87 centipoises for the egg white. The standard deviation between samples was 64.67 centipoises for egg white and 517.2 centipoises for egg yolk. Appendix C shows the raw data obtained for each viscosity reading. According to the literature, the viscosity of human mucoid effusion can range from 4 centipoises up to 32,000 centipoises [21, 23].

To analyze the viscosity values, Minitab statistical software (Minitab Release 14, State College, PA), specifically ANOVA (Analysis of Variance) was used. This program was used to determine if there was a significant difference between the viscosity values

depending on the length of time out of the refrigerator. Furthermore, an analysis was performed to determine if there was a significant difference between each sample over the five minute interval and if there was a significant difference between the viscosity values of different eggs. See Appendix D for the normal probability plots and statistical results. The simplified results are listed in Table 4-1.

Table 4-1: ANOVA analysis for significance.

Sample	**P value (< 0.05 is significant (*))**
Egg White: Viscosity Values vs. Time out of the Refrigerator	0.000
Egg White: Viscosity Values vs. Five Minute Interval	0.976
Egg White: Viscosity Sample 1 vs. Viscosity Sample 2	0.000
Egg Yolk: Viscosity Values vs. Time out of the Refrigerator	0.000
Egg Yolk: Viscosity Values vs. Five Minute Interval	0.992
Egg Yolk: Viscosity Sample 1 vs. Viscosity Sample 2	0.000

The results were also graphed for a typical egg sample to establish a trend in the changing viscosity over time out of the refrigerator. Figure 4.1 shows that the viscosity of egg yolk is not constant over time and gradually increases as it changes temperature.

Similarly, egg white viscosity increases and then decreases over time and the temperature increases. Figure 4-2 shows the change in egg white viscosity as a function of time out of the refrigerator.

Syringe Pump Calibration

A syringe pump was designed and built in order to deliver mucus through the tympanostomy tube.

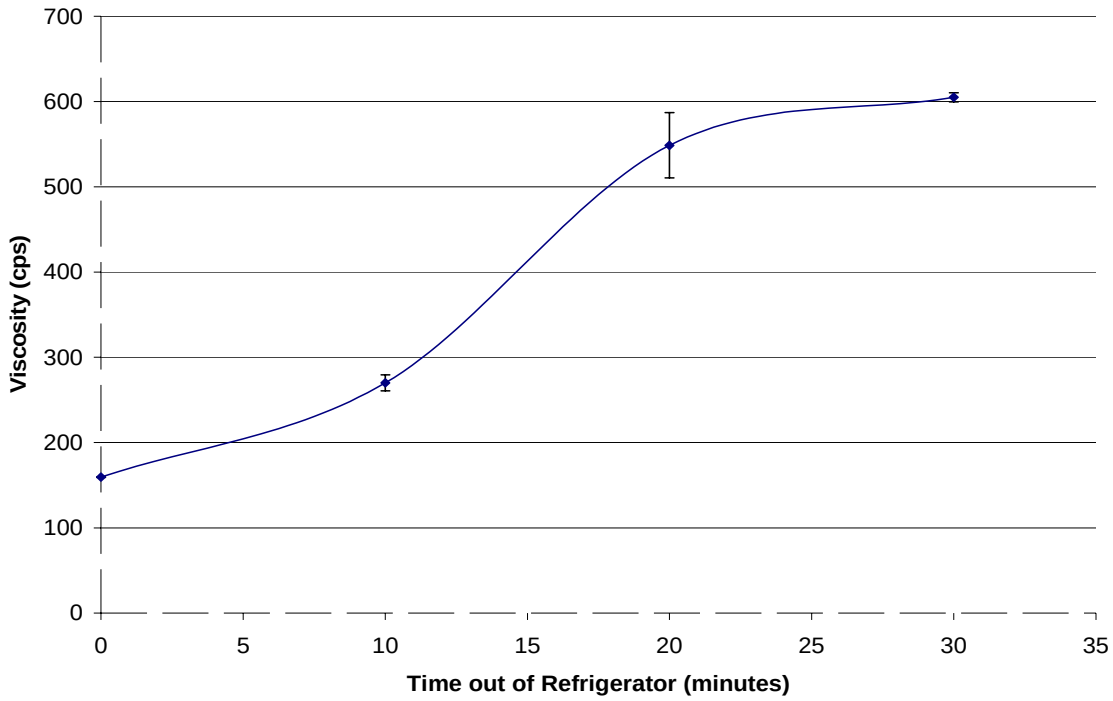

Figure 4-1: Change in viscosity of egg yolk over time.

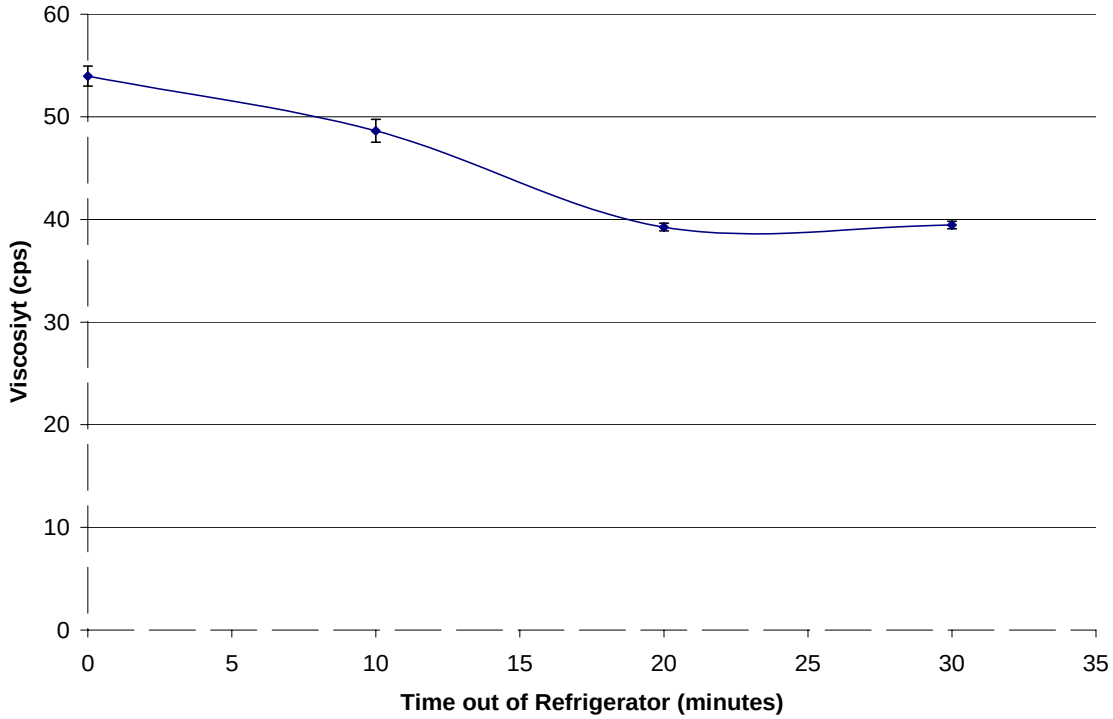

Figure 4-2: Change in viscosity of egg white over time.

The pump was driven by a stepper motor driver circuit that can vary the step rate of the motor. The step rate can be calibrated to accurately deliver mucus to the ear chamber and is controlled using the resistance control speed knob.

The calibration began by first adjusting the following settings. The rotation was set to clockwise (CW), the steps were set to ½ step, pin 9 was set in the on position, the step rate was set to continuous, the speed was set to slow, and the rate was set to the fastest setting. In addition, the shaft end of the stepper motor was connected to a ¼ inch round shaft coupling and then to a ¼ - 28 threaded screw. A ¼ - 28 threaded screw has 28 threads per inch which works out to a spacing of 0.035 inches between each thread. Therefore, each full rotation of the shaft corresponds to a lateral distance of 0.035 inches.

Following this, the time required for the shaft to complete one revolution was measured to be 10.66 minutes. In addition the flow rate for the syringe pump with these settings was 0.01ml/6 min. See Appendix E for a detailed look at the flow rate calculations.

Load Cell Calibration

The load cell used in this experiment outputs a voltage signal depending on the force applied. The voltage is proportional to the deformation of the Wheatstone bridge sensor. However, this output must be correlated to a specific force value. This was achieved by setting up a weight system. Several led weights were collected and placed on top of the load cell. As the weight gradually increases the resulting output voltage decreases. The associated voltage can then be related to the change in weight on the sensor. Appendix F shows the raw data obtained from each experiment. A linear regression was then applied to the graphed results and an equation was obtained (Figure 4-3). This equation can then be used to make a correlation between the voltage and force.

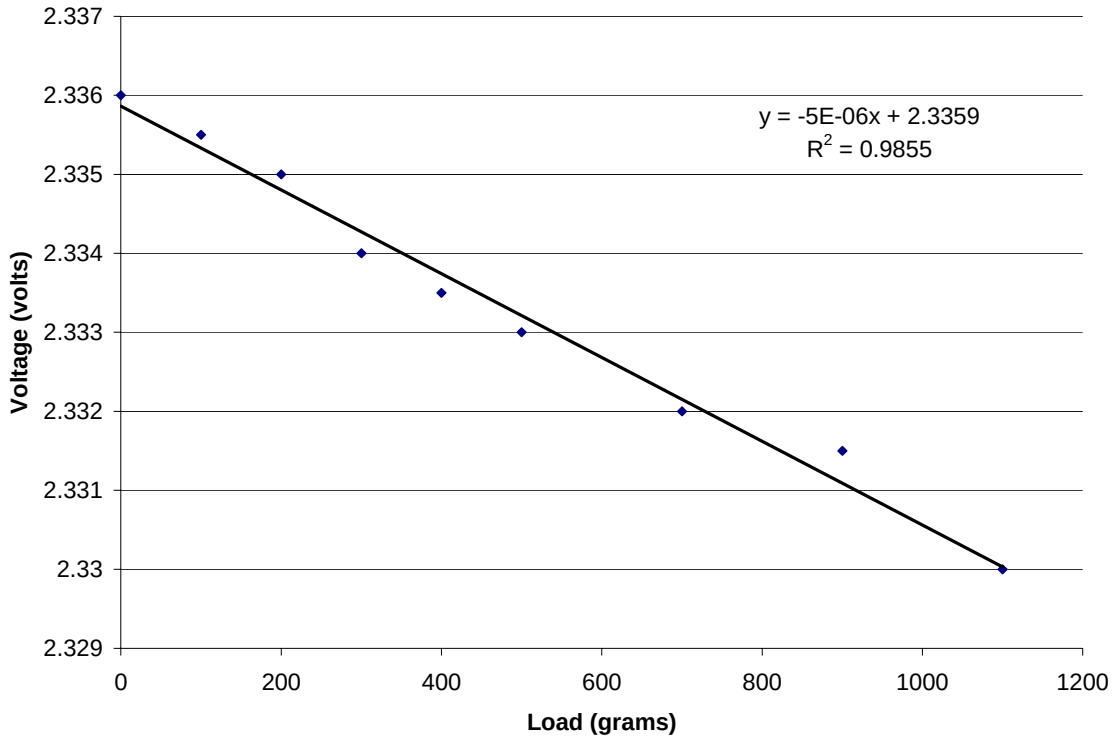

Figure 4-3: Calibration curve for load cell with trend line and equation.

CHAPTER 5
RESULTS

The incidence of tube occlusions is determined by the periodic plugging and clearance within the tube. A tube occlusion is explained by any increase in slope, of the accumulation of force graph, lasting approximately 5 minutes. Conversely, a clearance or expulsion of an occlusion is explained by the leveling or zero slope of the accumulation of force graph lasting approximately 3-5 minutes. The plugs are expelled from the tube when enough pressure builds up in the chamber.

Tube performance is assessed by measuring the subsequent time required for an occlusion to form and clear within the tube. However, over the course of each experiment, the tubes go through about seven cycles of occluding and clearing. Therefore, it is important to explain why the incidence of occlusion is so high and why some of the cycles are ignored during analysis. When analyzing the effect of length on the rate of reoccurrence of occlusions, it is important to eliminate as many variables as possible to isolate just the effects of length. Since the egg yolk is taken from a refrigerated environment and then tested, it gradually increases in temperature until it reaches room temperature (25°C). However, in chapter 4 it was shown that the viscosity of the yolk changes as the temperature (time out of the refrigerator) increases. Therefore, only cycles (occlusions) that occur after ~50-60 minutes, when the egg yolk has reached room temperature, will be investigated during analysis. In addition, the composition of the yolk is not uniform and contains "chunks". These chunks, although small and less common than those found in human mucus or egg white, can be attributed to some of the

occlusion cycles. Since the primary method of occlusion we would like to achieve would be the result of direct drying, the effects of the "chunks" can be minimized by looking at cycles occurring after 50-60 minutes when the yolk begins to noticeably dry in air. Before 50 minutes, the yolk has not had the appropriate time to dry and form an occlusion and false positives, such as chunks passing through the tube, overpower the effects of natural drying.

The typical accumulative force per increment graphs that are obtained after each experiment show the progression of force buildup over time. As shown in Figure 5-1, there is a difference in the time required for an occlusion to from and be expelled between the 12 mm long and 4.8 mm long tubes. An ANOVA test was conducted using MINITAB statistical analysis program. The results show in Figure 5-2 that there is a significant difference in the formation and clearance time between the 12mm (23 minutes) and 4.8mm (13.5 minutes) tubes, with equal diameter. The p-value was 0.021 (P-value < 0.05 is considered significant). See Appendix G and H for the MINITAB results and incidence of occlusions.

The method of occlusion is also examined. Occlusion can either occur within the tube, at the exit of the tube or at the entrance of the tube in the middle ear space. After each experiment was completed, the tube was examined. It was noted that all of the tubes occlude as a result of the gradual drying and subsequent buildup of yolk at the exit of the tube.

Over time, this buildup prevents mucus from exiting and causes a blockage. This blockage can be seen because the majority of the mucus is dried and on the external part

of the chamber. Mucus within the chamber does not dry as quickly, since it is not in direct contact with the outside air and is in constant contact with fresh mucus.

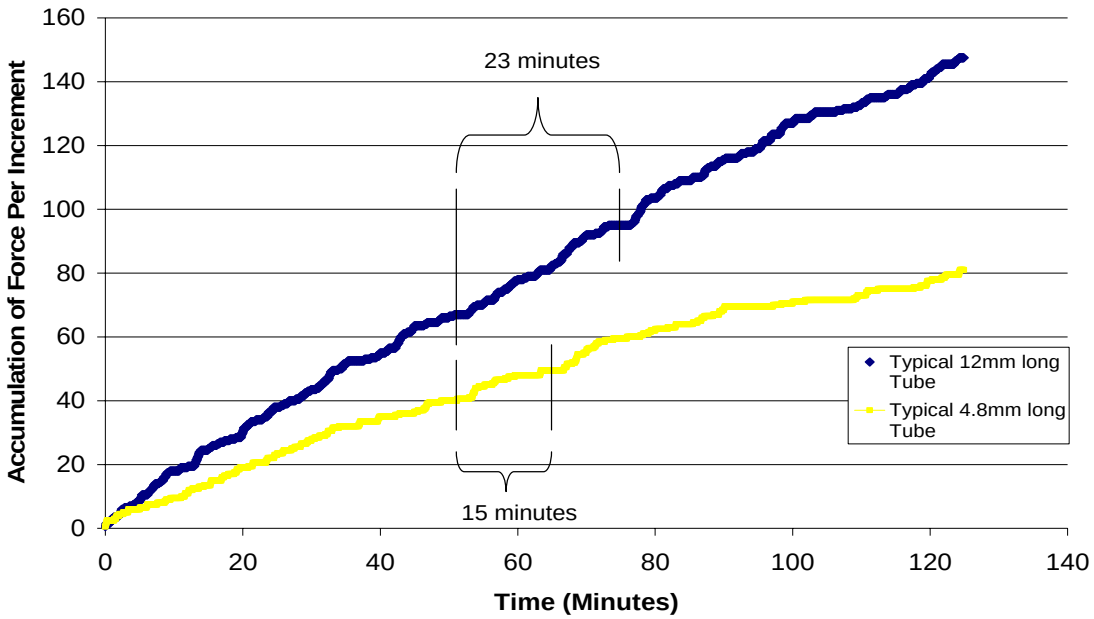

Figure 5-1: Effect of tube length on the rate of time required for an occlusion to form and expel out of Richard's T-tubes with the same inner diameter.

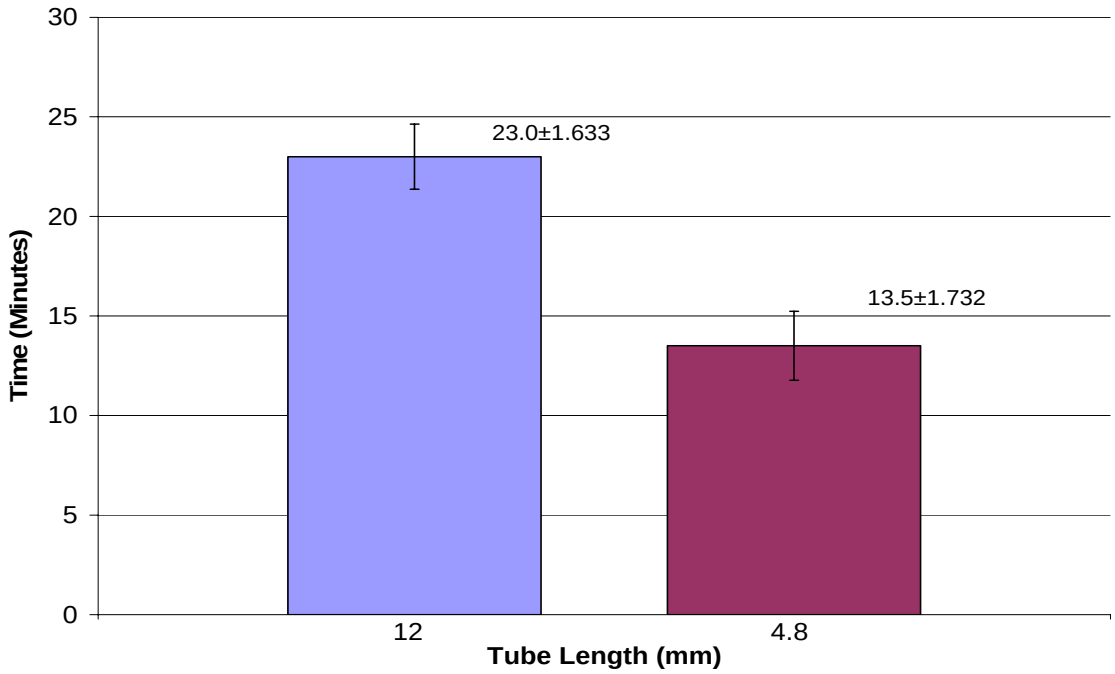

Figure 5-2: Effect of tube length on the time required for the formation and clearance of an occlusion. (P-value = 0.021, n = 8)

CHAPTER 6
SUMMARY AND CONCLUSIONS

The objective of this study was to develop an ear chamber that analyzes tube occlusions in tympanostomy tubes. In addition, this study utilized a mucus analog and data acquisition system to model the ear environment which allowed for a quantitative measurement of tube occlusion.

The experimental results presented in this research suggest that the in-vitro ear chamber can be used to analyze tube occlusions. The ability to isolate a single variable and test for the effects of that variable were proved. As a result, the chamber can be used to study the effects of coatings, geometry, and composition with fewer variables then in-vivo studies. This is verified through the discovery of the significant difference between the times required to form and unplug an occlusion based on tube length. Specifically, the results show that the 12mm tubes require a longer time than the 4.8mm tubes. This is the direct result of the increase in the fluid resistance within the longer tubes. Furthermore, the conclusions are consistent with the results calculated using the velocity profile and Poiseuille's Equation for mucus flowing through a cylindrical tube (Appendix I). The results of Poiseuille's Equation state that the flow rate is proportional to the change in pressure within the tube and is inversely proportional to the length. Therefore, if the flow rate is constant and the length of the tube is increased then the corresponding pressure gradient must increase. However, the rate of pressure increase is the same in both tubes, so more time is needed to reach the higher pressure required for the longer

tubes. Thus, the time required to expel the plug in the longer tubes is extended. See Appendix I for complete details.

In addition, another unique aspect of this project is that the fluid used to simulate human mucus was egg yolk. As it turns out the egg yolk yields the same results as predicted with the Poiseuille Equation yet is available in larger quantities and is easier to obtain than human mucus. Furthermore, the data acquisition system was able to repeatedly recreate the in-vivo environment of the ear, further decreasing the number of variables.

CHAPTER 7
FUTURE WORK

The results of this study indicate that length plays an important role in preventing occlusions. However, more research can be conducted to ultimately assess the best combination of length and composition that will demonstrate the lowest occlusion rate. Two additional factors that affect tube plugging are tube geometry and coatings. Experiments should be performed to determine their influence. Additionally, the experiments performed for this report were executed using egg yolk as a substitute for human mucoid effusion. It would be important to run the same experiments using human mucoid effusions to accurately mimic the in-vivo environment.

Further research towards an optimal chamber design to promote cleaning and prevent contamination is crucial when using human mucus. In addition, more precise methods for measuring the change in force within the chamber using Labview will increase the accuracy of the results. Plus, a larger sample size should be used to decrease the variability in the results. The automation of the system can be improved by connecting the stepper motor driver directly to the Labview program to reduce variables. Moreover, determining the rheological properties of the human mucoid effusions would be crucial to understanding possible modes of occlusion as well as determining a starting point for discovering additional mucus analogs. Therefore, future research should include discovering a method for measuring the viscosity, as well as viscoelasticity of human mucoid effusions.

APPENDIX A
LABVIEW PROGRAM

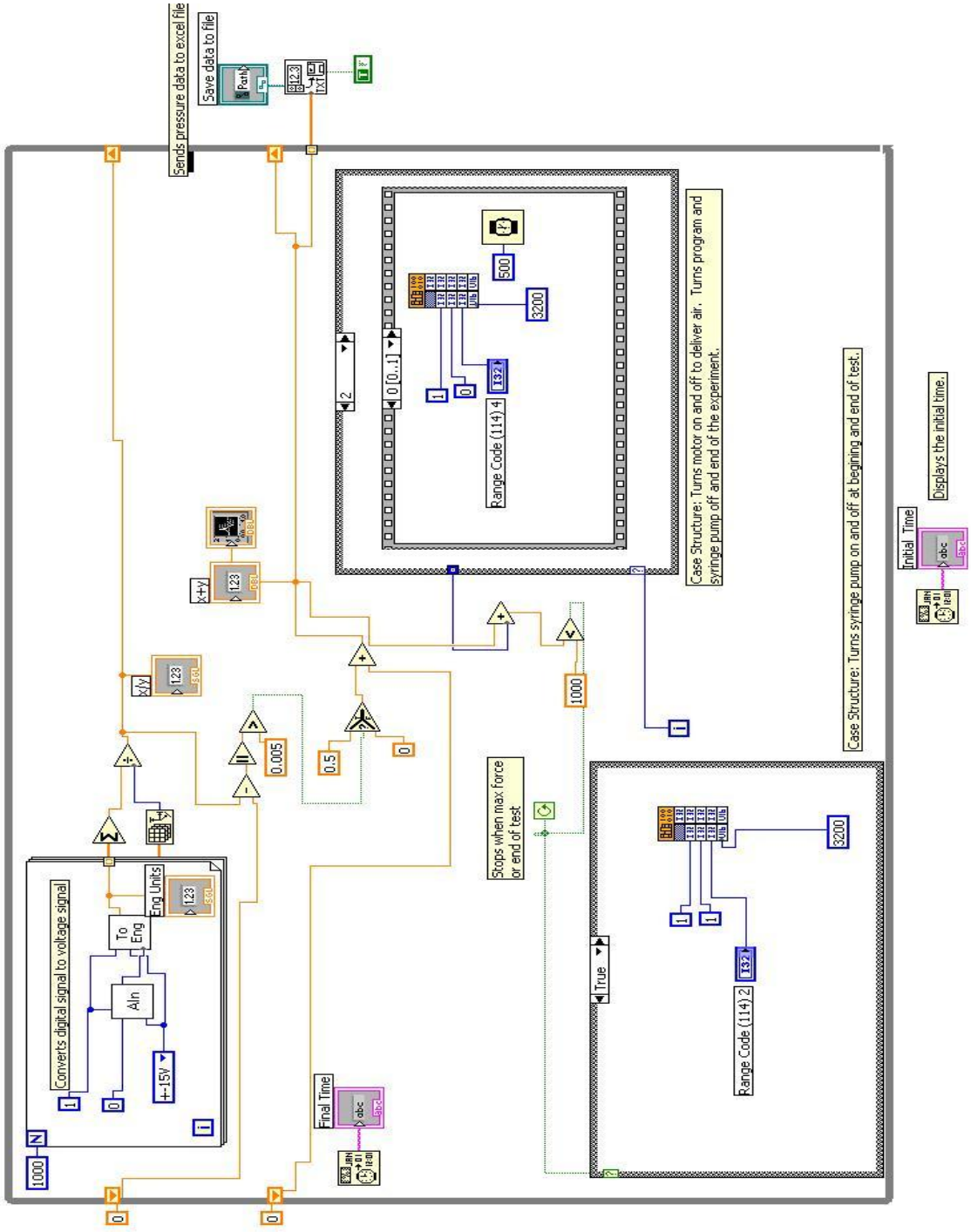

APPENDIX B
BROOKFIELD VISCOMETER

The viscometer works by spinning a fluid sample between a cone and plate (Figure D-1). The operating principle of the viscometer is that a conical spindle rotates at a precise speed as the torque necessary to overcome the viscous resistance is measured. This is achieved by passing the spindle through a calibrated beryllium copper spring. A rotational transducer is then used to determine the degree to which the spring was wound. This spring displacement is directly proportional to the viscosity of the fluid.

The theory behind the operation of the viscometer is that of uniform shear. The axis of a conical surface is aligned perpendicular to a flat plate, with the peak of the cone lying on the surface of the plate (Figure D-1). If the cone is rotated, then the fluid in the space between the two will be subjected to a uniform shear rate. This means that the rate of movement of a particle within the flow is proportional to its distance away from the axis as well as the separation distance at that point. In addition, the ratio of the distance of separation and rate of movement for any speed is constant over the surface. Furthermore, by using small angles, (less than 4°) shearing stresses can be achieved with low rotational speeds, viscosities, and sample sizes [25]. In addition, the degree of the cone is very obtuse with an angle (θ) of less than 4° and the cone is rotated at a constant speed (ω).

The viscosity (Equation D-5) is therefore determined by the ratio of the shear stress to the shear rate. The shear stress (Equation D-3) is associated with the summation of the torque (T) over the conical surface whereas the shear rate (Equation D-4) is related to the

rotational speed (ω) of the cone and the gap width (d) at a distance (r) away from the center of the cone. In addition, since (d) and (ω) are constants and (d) is a maximum at a radius of (r) then the sheer rate is related to (ω) and sin θ. The mathematical relationships are listed below.

$$\text{Torsional Shear Stress} = \tau = \frac{T}{J} \qquad \text{Equation D-1}$$

T = % Full scale torque (dyne-cm)

J = Polar moment of inertia

$$\text{For a cone: } J = \frac{2}{3}\pi r^3 \qquad \text{Equation D-2}$$

Plugging in Equation D-2 into Equation D-1 gives

$$\text{Shear Stress (dynes/cm}^2\text{)} = \tau = \frac{T}{\frac{2}{3}\pi r^3} \qquad \text{Equation D-3}$$

$$\text{Shear Rate (sec}^{-1}\text{)} = \gamma = \frac{\omega}{\sin\theta} \qquad \text{Equation D-4}$$

$$\text{Viscosity (Centipoise) (mPa s)} = \nu = \frac{\tau \cdot 100}{\gamma} \qquad \text{Equation D-5}$$

r = Cone radius (cm)

ω = Cone speed (rad/sec)

θ = Cone angle (degrees)

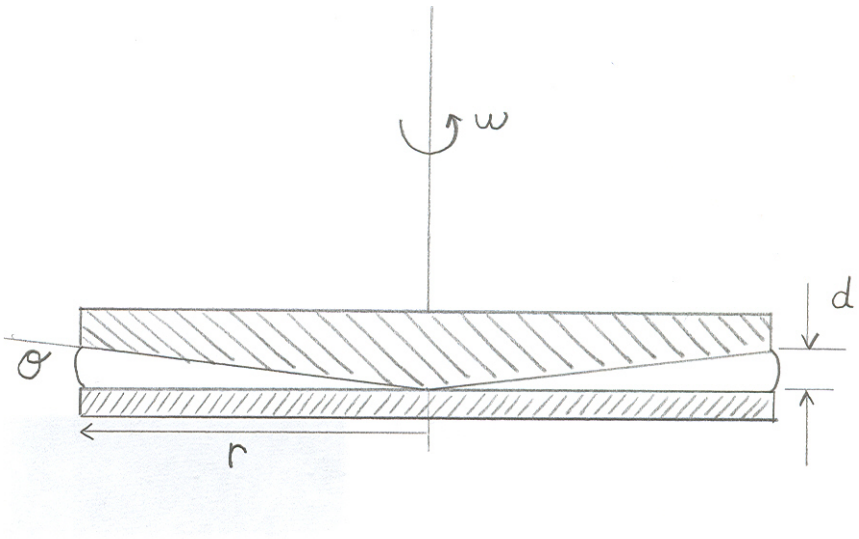

Figure D-1: Schematic of cone and plate viscometer.

APPENDIX C
EGG YOLK/WHITE VISCOSITY MEASUREMENTS

Table C-1: Viscosity measurements of egg yolk test #1 @ 10 RPM

Test #	**Viscosity @ 2 min**	**Viscosity @ 4 min**	**Viscosity @ 5 min**	**Time out of Refrigerator (min)**
1	160	159.36	159.36	0
2	278.4	272	259.84	10
3	522.24	592.64	531.2	20
4	611.2	602.24	601.6	30
Average Viscosity (cps)	**392.96**	**406.56**	**388**	

Table C-2: Viscosity measurements of egg yolk test #2 @ 1 RPM

Test #	**Viscosity @ 2 min**	**Viscosity @ 4 min**	**Viscosity @ 5 min**	**Time out of Refrigerator (min)**
1	1382.4	1369.6	1369.6	0
2	1555.2	1574.4	1548.8	10
3	1209.6	1196.8	1184	20
4	697.6	684.8	672	30
Average Viscosity (cps)	**1211.2**	**1206.4**	**1193.6**	

Table C-3: Viscosity measurements of egg white test #1 @ 10 RPM (Factor 640)

Test #	**Viscosity @ 2 min**	**Viscosity @ 4 min**	**Viscosity @ 5 min**	**Time out of Refrigerator (min)**
1	53.12	53.76	55.04	0
2	49.28	47.36	49.28	10
3	39.04	39.04	39.68	20
4	39.68	39.04	39.68	30
Average Viscosity (cps)	**45.28**	**44.8**	**45.92**	

Table C-4: Viscosity measurements of egg white test #2 @ 10 RPM (Factor 640)

Test #	**Viscosity @ 2 min**	**Viscosity @ 4 min**	**Viscosity @ 5 min**	**Time out of Refrigerator (min)**
1	147.2	145.28	153.6	0
2	185.6	179.2	182.4	10
3	165.76	154.24	154.88	20
4	167.68	156.16	156.8	30
Average Viscosity (cps)	**166.56**	**158.72**	**161.92**	

APPENDIX D
EGG VISCOSITY STATISTICS

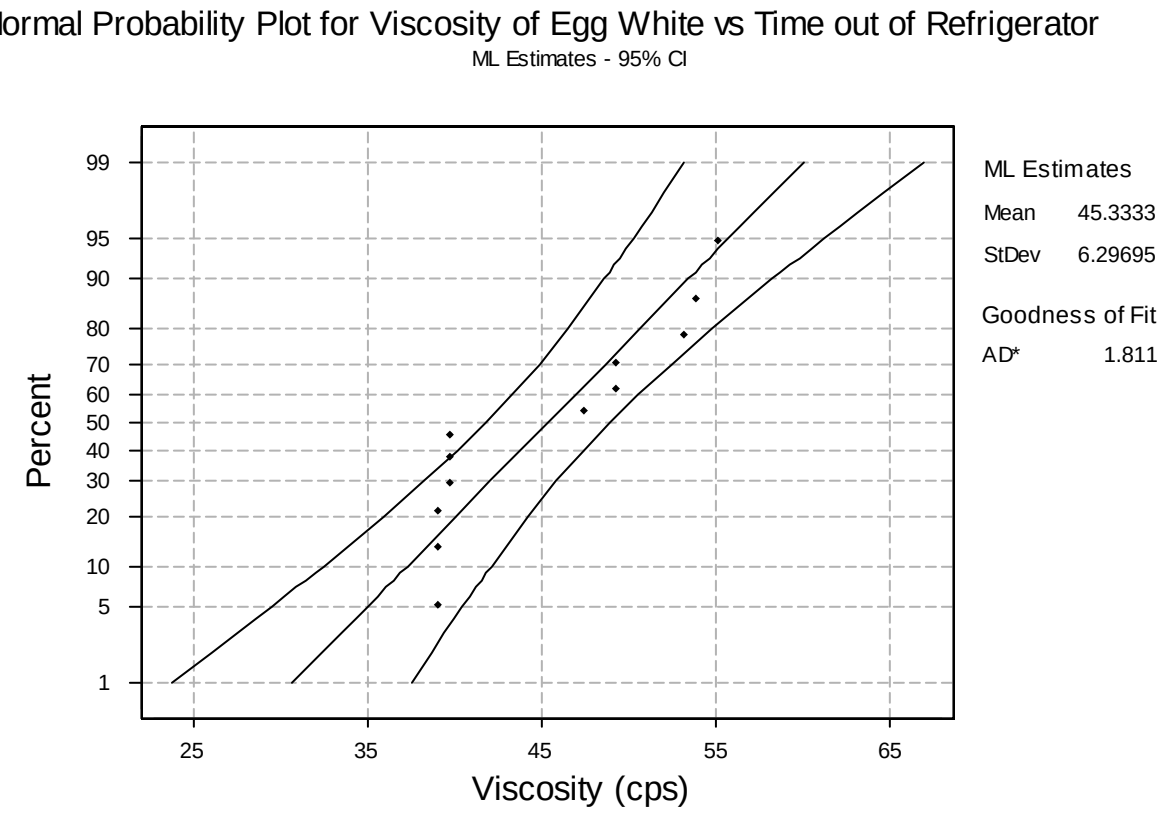

One-way ANOVA: Viscosity of Egg White vs. Time out of Refrigerator

```
Analysis of Variance for Visc. wh
Source     DF        SS        MS        F        P
time out    3   470.903   156.968   255.48    0.000
Error       8     4.915     0.614
Total      11   475.819

                                 Individual 95% CIs For Mean
                                 Based on Pooled StDev
Level       N      Mean     StDev  ----+---------+---------+---------+--
0 min       3    53.973     0.978                                 (-*-)
10 min      3    48.640     1.109                       (-*-)
20 min      3    39.253     0.370  (--*-)
30 min      3    39.467     0.370   (-*-)
                                 ----+---------+---------+---------+--
Pooled StDev =    0.784           40.0      45.0      50.0      55.0
```

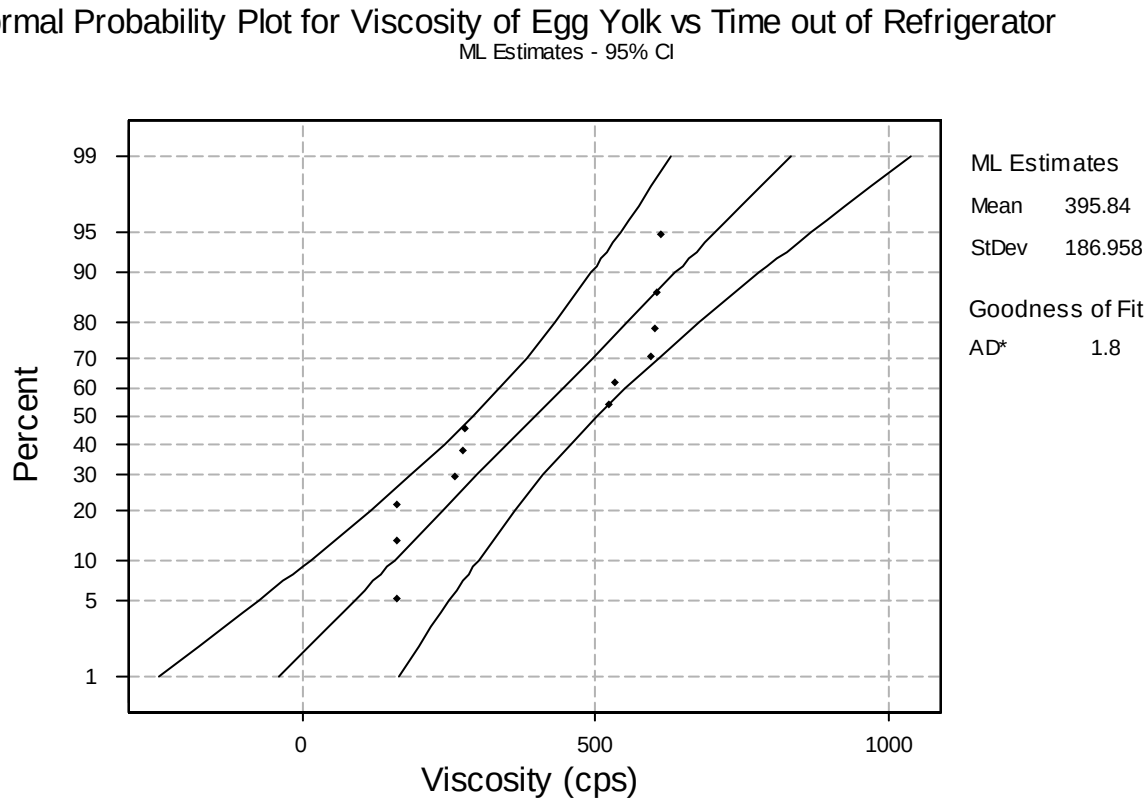

One-way ANOVA: Viscosity of Egg Yolk vs. Time out of Refrigerator

```
Analysis of Variance for Visc. yo
Source     DF        SS        MS        F        P
time out    3    416265    138755   349.87    0.000
Error       8      3173       397
Total      11    419438

                                    Individual 95% CIs For Mean
                                    Based on Pooled StDev
Level       N      Mean     StDev  --+---------+---------+---------+----
0 min       3    159.57      0.37   (-*)
10 min      3    270.08      9.43          (-*-)
20 min      3    548.69     38.32                              (-*)
30 min      3    605.01      5.37                                  (*-)
                                    --+---------+---------+---------+----
Pooled StDev =    19.91             150       300       450       600
```

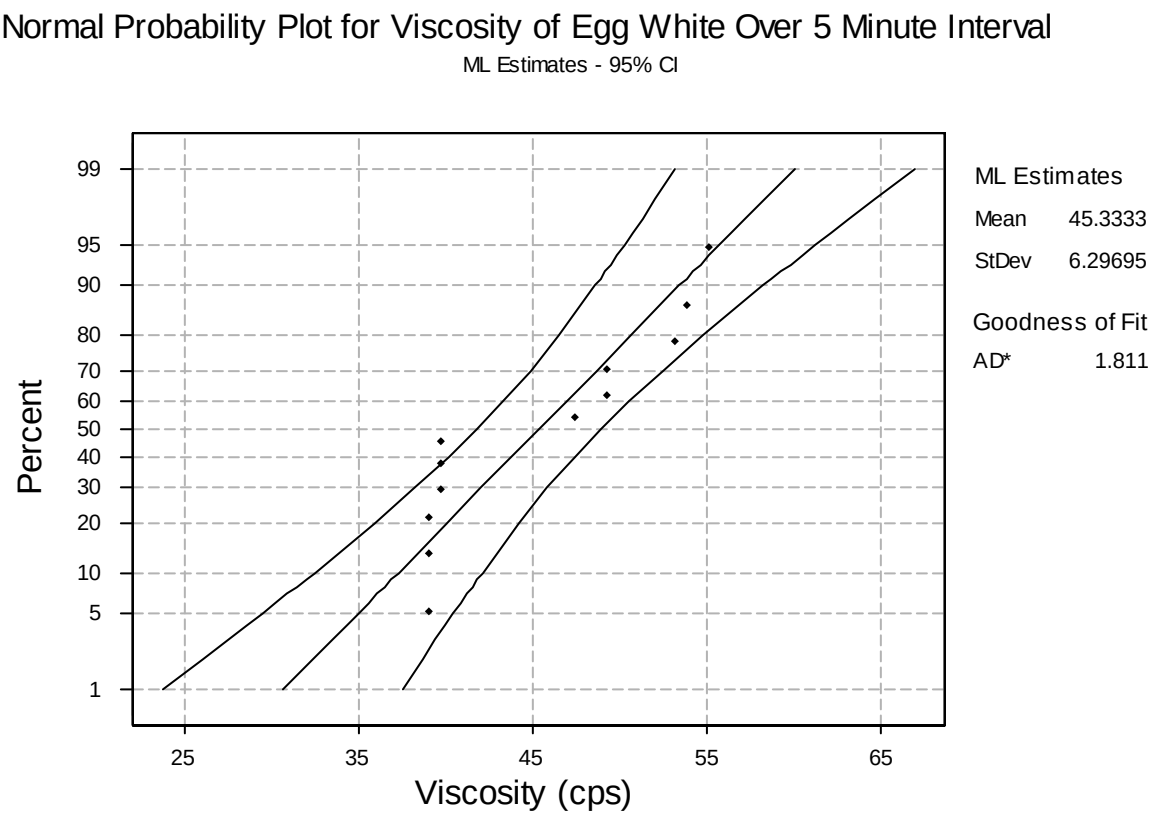

One-way ANOVA: Viscosity of Egg White vs. 5 Minute Interval

```
Analysis of Variance for 5 y int
Source     DF        SS        MS        F        P
time 5      2       741       371     0.01    0.992
Error       9    418791     46532
Total      11    419532

                                  Individual 95% CIs For Mean
                                  Based on Pooled StDev
Level       N      Mean     StDev  -+---------+---------+---------+-----
2 min       4     392.9     209.6   (---------------*---------------)
4 min       4     406.6     225.2    (---------------*---------------)
5 min       4     388.0     212.0   (---------------*---------------)
                                  -+---------+---------+---------+-----
Pooled StDev =    215.7           150       300       450       600
```

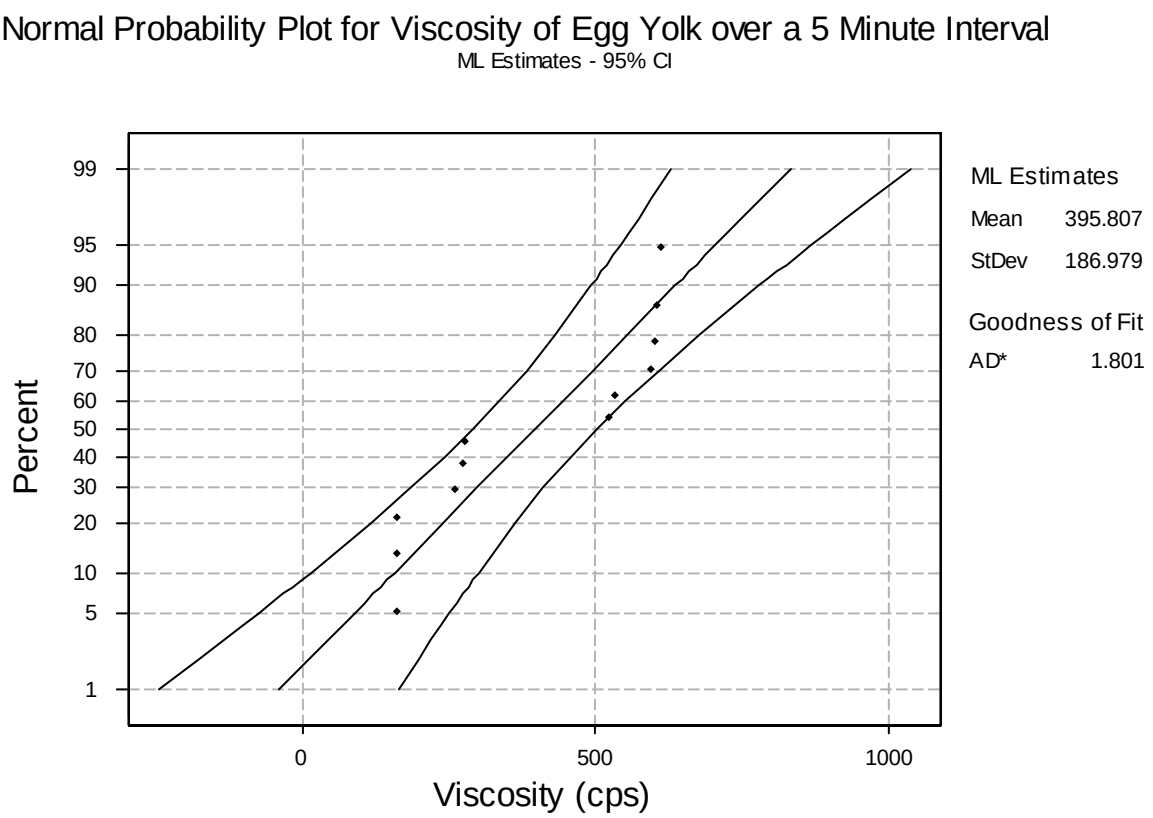

One-way ANOVA: Viscosity of Egg Yolk vs. 5 Minute Interval

```
Analysis of Variance for 5 w int
Source     DF        SS        MS        F        P
time 5      2       2.5       1.3     0.02    0.976
Error       9     473.3      52.6
Total      11     475.8

                                  Individual 95% CIs For Mean
                                  Based on Pooled StDev
Level       N      Mean     StDev  -------+---------+---------+---------
2 min       4    45.280     7.018   (----------------*---------------)
4 min       4    44.800     7.146  (----------------*---------------)
5 min       4    45.920     7.579    (----------------*---------------)
                                  -------+---------+---------+---------
Pooled StDev =    7.252              40.0      45.0      50.0
```

One-way ANOVA: Viscosity of Egg Yolk Between Two Different Samples

```
Analysis of Variance for yolk to
Source     DF        SS        MS        F        P
Sample      1   2211762   2211762  8.1E+04    0.000
Error       4       109        27
Total       5   2211872

                                  Individual 95% CIs For Mean
                                  Based on Pooled StDev
Level       N      Mean     StDev  ------+---------+---------+---------+
1           3    159.57      0.37  (*
2           3   1373.87      7.39                                    *
                                  ------+---------+---------+---------+
Pooled StDev =     5.23               350       700      1050      1400
```

One-way ANOVA: Viscosity of Egg White Between Two Different Samples

```
Analysis of Variance for white to
Source     DF        SS        MS        F        P
Sample      1  13457.82  13457.82  1350.25    0.000
Error       4     39.87      9.97
Total       5  13497.69

                                  Individual 95% CIs For Mean
                                  Based on Pooled StDev
Level       N      Mean     StDev  ----+---------+---------+---------+--
1           3     53.97      0.98  (-*-)
2           3    148.69      4.36                                  (-*)
                                  ----+---------+---------+---------+--
Pooled StDev =     3.16              60        90       120       150
```

APPENDIX E
SYRINGE PUMP CALIBRATION

The time required for the shaft to complete one revolution was measured and then averaged after several runs. Table E-1 shows the raw data obtained from all of the tests.

Table E-1: Syringe pump calibration data.

Test #	Slowest Speed Setting Time for 1 Revolution (min)	Fastest Speed Setting Time for 1 Revolution (min)
1	11.0	8.7
2	10.5	8.7
3	10.5	8.6
Average	10.66	8.73

Furthermore, the flow rate was calculated by first solving for the radius of the syringe. The measured distance between each 0.1 ml tick mark was 15/64 inches (0.2343 inches). Therefore, the radius can be determined from Equation E-1.

$$\pi r^2 h = 0.1ml = 0.0061024in^3 \qquad \text{Equation E-1}$$

h = Height = 0.2342 inches

r = Inner radius

Therefore, if r = 0.0911 inches then the flow rate, using the fastest setting, can be determined from Equation E-2. Figure E-1 shows the calibration curve with a trend line representing how flow rate changes with syringe speed.

$$\pi r^2 h = (\pi)(0.0911)^2(0.035714) = 0.0009311in^3$$
$$0.0009311in^3 / 8.73\min = 0.015259ml / 8.73\min \qquad \text{Equation E-2}$$
$$Q = 0.00002913ml / \sec = 0.01ml / 6\min$$

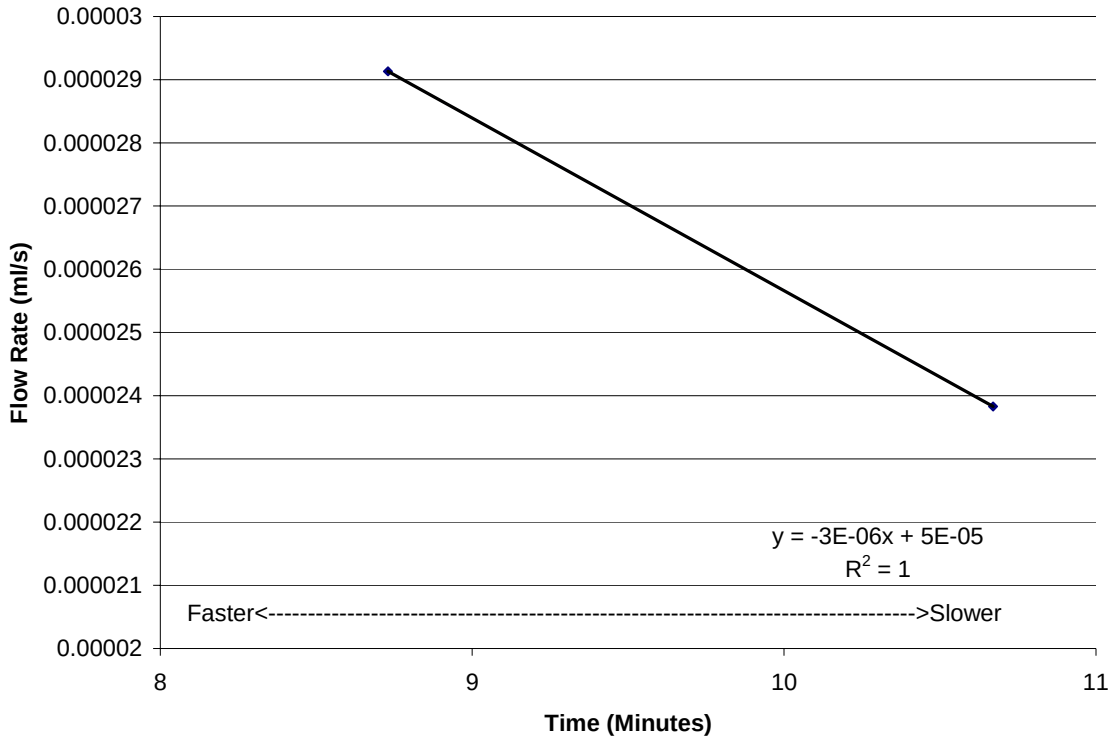

Figure E-1: Calibration curve for syringe pump with trend line and equation.

APPENDIX F
LOAD CELL CALIBRATION

In order to calibrate the load cell the voltage was measured as weight was added to the transducer. The corresponding voltage values were recorded after 10 seconds and the results are listed in Table F-1.

Table F-1: Calibration data for load cell transducer.

Weight (gram)	**Voltage (volts)**
0	2.336
100	2.3355
200	2.335
300	2.334
400	2.3335
500	2.333
700	2.332
900	2.3315
1100	2.330

APPENDIX G
OCCLUSION TIME VS LENGTH STATISTICS

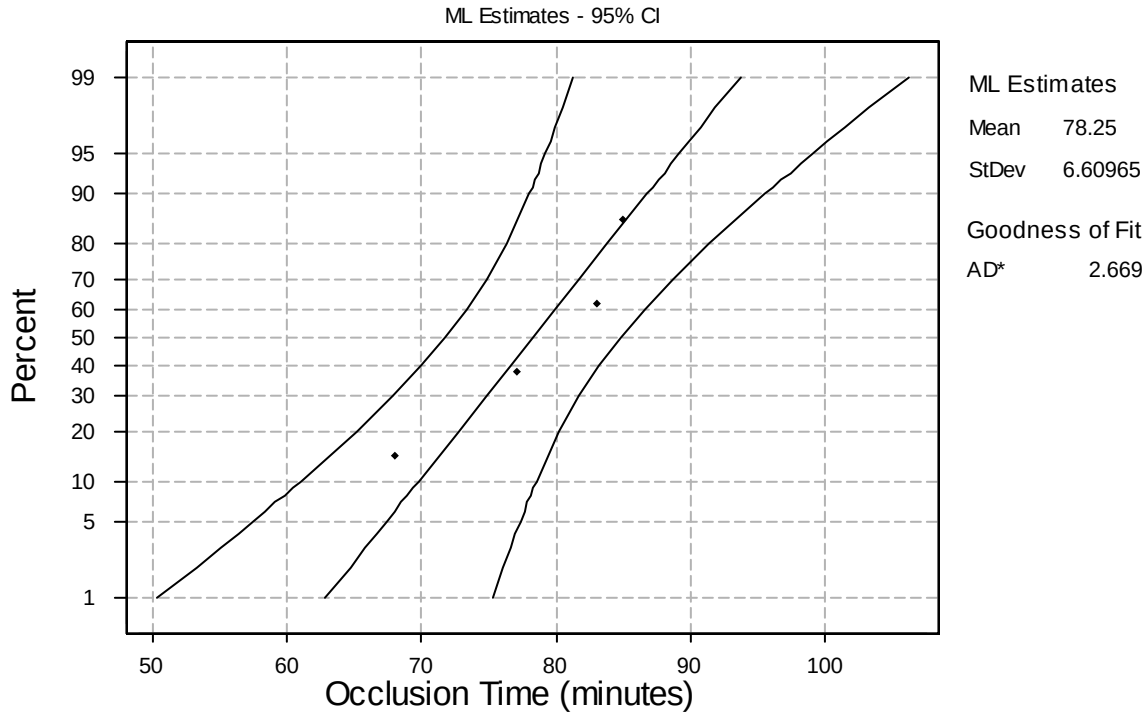

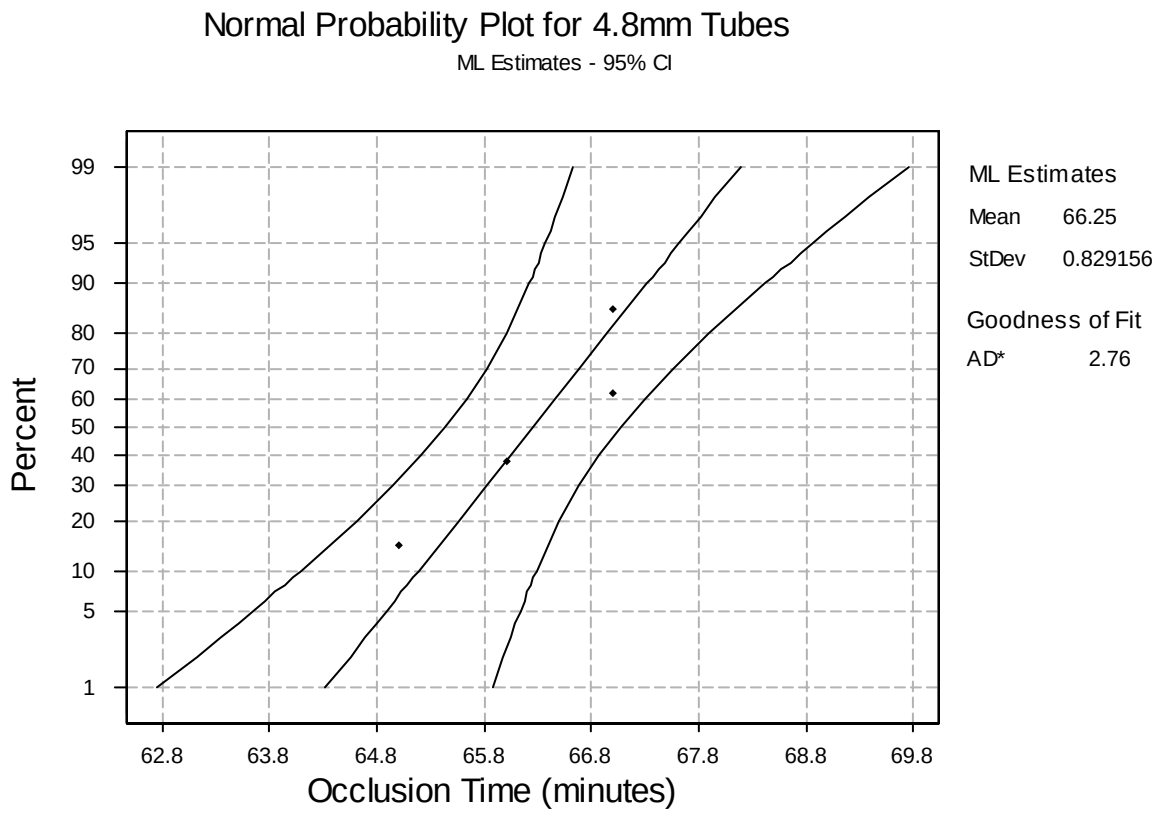

One-way ANOVA: Clearance Time versus Length

```
Analysis of Variance for Occlusio
Source     DF        SS        MS        F        P
Length      1     288.0     288.0     9.74    0.021
Error       6     177.5      29.6
Total       7     465.5

                                 Individual 95% CIs For Mean
                                 Based on Pooled StDev
Level       N      Mean     StDev  -----+---------+---------+---------+-
12mm        4    78.250     7.632                  (---------*--------)
4.8mm       4    66.250     0.957  (---------*--------)
                                   -----+---------+---------+---------+-
Pooled StDev =    5.439              63.0      70.0      77.0      84.0
```

APPENDIX H
INCIDENCE OF OCCLUSIONS

The length of time it takes for an occlusion to form and expel from the tube is recorded based on the stated methods. The results of each test are listed in Table H-1.

Table H-1: Effect of length on the time required for an occlusion to form and expell.

Sample #	Sample Length (mm)	Time (minutes)	Average Time (minutes)	Standard Deviation (+/-)
1	4.8	15	13.5	1.73
2	4.8	12		
3	4.8	12		
4	4.8	15		
1	12	21	23	1.63
2	12	25		
3	12	23		
4	12	23		

APPENDIX I
VELOCITY PROFILE/ POISEUILLE'S EQUATION

In order to calculate the Poiseuille Equation the velocity profile must be found for a fluid flowing through a cylinder. In computing the velocity profile it is assumed that the flow is fully developed and laminar. To prove this the Reynolds number and entrance length are calculated. If the egg yolk can be modeled as an incompressible Newtonian fluid, then the Reynolds number [26] can be described as:

$$\begin{aligned} &\mathrm{Re} = \frac{\rho V D}{\mu} \\ &\rho = 1.035 g/cm^3 \\ &V = Q/A \\ &D = 1.14 mm \\ &\mu = 400 cps = 4.0 g/cm \cdot s \end{aligned} \qquad \text{Equation I-1}$$

Where ρ is the density of the egg yolk, V is the velocity of the fluid, D is the diameter of the tube, and μ is the viscosity of the egg yolk. The density was found in literature [27]. The Diameter is measured from the tube. The viscosity is taken from experimental measurements. The velocity can be calculated from the volumetric flow rate (Q) and the area (A). Equation I-2 gives the equation for the velocity.

$$V = \frac{Q}{A} = \frac{1.747 mm^3/\min}{1.0207 mm^2} = 1.7115 mm/\min \qquad \text{Equation I-2}$$

The Reynolds number is then.

$$\mathrm{Re} = \frac{\left(\frac{1.035 g}{cm^3}\right)\left(\frac{0.002852 cm}{s}\right)(0.114 cm)}{\frac{4.0 g}{cm \cdot s}} = 0.00008412 \qquad \text{Equation I-3}$$

Since the Reynolds number is less than 2300 then the entrance length can then be calculated [26]

$$L = 0.06\,\mathrm{Re}\cdot D$$
$$L = 0.06(0.00008412)(1.14mm) = 0.0000057542mm \qquad \text{Equation I-4}$$

Therefore, since the entrance length is small and the flow is fully developed at the exit, then the velocity profile can be determined with the following assumptions.

- Steady
- Incompressible
- Neglect Body Force
- 2-D Flow
- No-slip Boundary Condition
- Solid Walls

Under these conditions the Navier Stokes equation in the direction of flow simplifies into

$$\frac{1}{r}\frac{\partial}{\partial r}(r\tau_{rz}) = \frac{\partial P}{\partial z} \qquad \text{Equation I-5}$$

After integrating with respect to r and since $\tau_{yz} = \mu\frac{\partial u}{\partial r}$, the velocity profile becomes.

$$u = \frac{r^2}{4\mu}\frac{\partial P}{\partial z} + \frac{C_1}{\mu}Ln(r) + C_2 \qquad \text{Equation I-6}$$

Plugging in the boundary conditions

- @ r = 0 velocity is finite => C_1=0
- @ r = R no slip; u = 0 => $C_2 = -\frac{R^2}{4\mu}\frac{\partial p}{\partial x}$

The velocity profile can be rewritten as:

$$u = \frac{R^2}{4\mu}\frac{\partial P}{\partial z}\left[1-\left(\frac{r}{R}\right)^2\right] \qquad \text{Equation I-7}$$

Once the velocity profile has been determined a relationship between pressure and flow rate was discovered (Equation I-8)

$$Q = \int_A V \cdot dA = \int_0^R u 2\pi r dr \qquad \text{Equation I-8}$$

After some substitution and manipulation the resulting Poiseuille equation is as follows.

$$Q = \frac{\pi D^4}{128\mu}\frac{\Delta P}{L} \qquad \text{Equation I-9}$$

Therefore, if the flow rate is constant and the length of the tube increases, the change in pressure must increase.

LIST OF REFERENCES

1. Armstrong, B.W., A new treatment for chronic secretory otitis media. Arch. Otolaryngol, 1954. 59: p. 653-654.

2. Shone, G.R., Griffith, I.P., Titanium grommets: a trial to assess function and extrusion rates. The Journal of Laryngology and Otology, 1990. 104: p. 197-199.

3. Tarek, J.S., Avoidance of postoperative blockage of ventilation tubes. The Laryngoscope, 1995. 105: p. 833-834.

4. Westine, J.G,. Giannoni, C.M., Antonelli, P.J., Defining tympanostomy tube plugs. The Laryngoscope, 2002. 112: p. 951-954.

5. Altman, J.S., Haupert, M.S., Hamaker, R.A., Belenky, W.M., Phenylephrine and the prevention of postoperative tympanostomy tube obstruction. Arch. Otolaryngol Head Neck Surg., 1998. 124: p. 1233-1236.

6. Cunningham, M.J., Harley, E.H., Jr., Preventing perioperative obstruction of tympanostomy tubes: a prospective trial of a simple method. International Journal of Pediatric Otorhinolaryngology, 1991. 21: p. 15-20.

7. Arnold, D.J., Bressler, K.L., Permeability of tympanotomy tubes to ototopical preparations. Otolaryngol Head Neck Surgery, 1999. 121: p. 35-37.

8. Ghosh, M.S., Kumar, W.C.N.A., Study of middle ear pressure in relation to eustachian tube patency. Ind. J. Aerospace Med., 2002. 46(2): p. 27-31.

9. Kinnari, T.J., Salonen, E., Jero, J., New method for coating tympanostomy tubes to prevent tube occlusions. International Journal of Pediatric Otorhinolaryngology, 2001. 58: p. 107-111.

10. Kinnari, T.J., Salonen, E., Jero, J., Durability of the binding inhibition of albumin coating on tympanostomy tubes. International Journal of Pediatric Otorhinolaryngology, 2003. 67: p. 157-164.

11. Kinnari, T.J., Jero, J., Kuusela, P., Yao, K., Okamoto, M., Experimental and clinical experience of albumin coating of tympanostomy tubes. Otolaryngol Head Neck Surgery, 2004. 131(2): p. 220.

12. Mehta, A.J., Stevens, G.R., Antonelli, P.J., Opening plugged tympanostomy tubes: effect of inner diameter and shaft length. Otolaryngol Head Neck Surgery, 2005. 132: p. 322-326.

13. Morris, M.S., Tympanostomy tubes: types, indications, techniques, and complications. Otolaryngologic Clinics of North America, 1999. 32(3): p. 385-389.

14. Oberman, J.P., Derkay, C.S., Posttympanostomy tube otorrhea. American Journal of Otolaryngology, 2004. 25(2): p. 110-117.

15. Roland, P.S., Stroman, D.W., Parry, D.A.,, Microbiology of acute otitis media with a tympanostomy tube. Otolaryngol Head Neck Surgery, 2004. 131(2): p. 49.

16. Roland, P.S., Kreisler, L., Reese, B., Topical ciprofloxacin/dexamethasone otic suspension is superior to ofloxacin otic solution in the treatment of children with acute otitis media with otorrhea through tympanostomy tubes. Annals of Emergency Medicine, 2004. 44(4): p. 431.

17. Rovers, M.M., Schilder, A.G., Zielhuis, G.A., Rosenfeld, R.M., Otitis media. Lancet, 2004. 363: p. 465-473.

18. Saidi, I.S., Biedlingmaier, J.F., Whelan, P., In vivo resistance to bacterial biofilm formation on tympanostomy tubes as a function of tube material. Otolaryngol Head Neck Surgery, 1999. 120: p. 621-627.

19. Tsao, B.A., Stevens, G.R., Antonelli, P.J., Opening plugged tympanostomy tubes: effect of tube compostion. Otolaryngol Head Neck Surgery, 2003. 128: p. 870-874.

20. Westine, J.G., Giannoni, C.M., Gajewski, B., Antonelli, P.J., Opening plugged tympanostomy tubes. The Laryngoscope, 2002. 112: p. 1342-1345.

21. Wiederhold, M.L., Zajtchuk, J.T., Vap, J.G., Paggi, R.E., Hearing loss in relation to physical properties of middle ear effusions. Ann. Otol. Rhinol. Laryngol., 1979: p. 185-189.

22. Witsell, D.L., Stewart, M.G., Monsell, E.M., Hadley, J.A., Terrell, J.E., Yueh, B., Rosenfeld, R.M., Hannley, M.T., Holzer, S.S., The cooperative outcomes group for ENT: A multicenter prospective cohort study on the outcomes of tympanostomy tubes for children with otitis media. Otolaryngol Head Neck Surgery, 2005. 132: p. 180-188.

23. Yagi, N., Fukazawa, T., Kurata, K., Honjo, I., A new microviscometer for determining the viscosity of middle ear effusion. American Journal of Otolaryngol, 1986. 4: p. 407-409.

24. Marieb, E.N., Human anatomy and physiology. 5th ed. 2001, San Francisco: Benjamin Cummings.

25. Brookfield, E.L. The wells-brookfield cone/plate digital viscometer. 1999, Stoughton: Brookfield Engineering Laboratories.

26. Fox, R.W., McDonald, A.T., Introduction to fluid mechanics. 5th ed. 1998, New York: John Wiley and Sons, Inc.

27. Vadehra, D.V., Nath, K.R., Eggs as a source of protein. CRC Critical Reviews in Food Technology, 1973. 4: p. 193-309.

BIOGRAPHICAL SKETCH

The author was born November 13, 1978, in New York City, New York, to an elementary school teacher and a secretary. He has one younger sibling, a very talented actress and artist, Nicole. After 18 months the author's parents moved to West Palm Beach, Florida. It was here that the author grew up and discovered the wonderful world of engineering. As a child he constantly took apart everything he could get his hands on and used the parts to create other inventions. It was here that he fell in love with science, a lifelong passion that is with him constantly. In May 2002 he received his Bachelor of Science in Engineering Science with a minor in biomechanics from the University of Florida and entered graduate school in the Mechanical Engineering Department. Shortly before finishing his bachelor's he started working for Dr. Roger Tran-Son-Tay in the Biorheology Lab and continues pursuing his research today. In the summer of 2001 he met his love of his life Amy and from then on knew that he had found his soul mate. On February 1, 2004, he asked her to marry him and on June 6, 2006, they will be married.